

行政院國家科學委員會專題研究計畫 期中進度報告

用於增進 MIMO-OFDM 系統性能之編碼與調變--總計畫(1/3) 期中進度報告(完整版)

計畫類別：整合型
計畫編號：NSC 95-2219-E-002-025-
執行期間：95年08月01日至96年07月31日
執行單位：國立臺灣大學電機工程學系暨研究所

計畫主持人：林茂昭
共同主持人：蘇炫榮、陸曉峯

處理方式：期中報告不提供公開查詢

中華民國 96 年 05 月 25 日

用於增進 MIMO-OFDM 系統 性能之編碼與調變(1/3)

Coding and Modulation For Enhancing Performances of MIMO- OFDM Systems (1/3)

執行期限：95/08/01~96/7/31

計畫編號：NSC 95-2219-E-002-025

計畫主持人：林茂昭

摘要

在本報告中我們將呈現三個子計畫第一年研究所得之豐碩成果。於第一個子計畫中我們建構出以成對錯誤率考量之下符合最佳分集多工交換 (diversity-multiplexing tradeoff) 之空頻碼。我們也建構出以碼字錯誤率考量之下符合最佳分集多工交換 (diversity-multiplexing tradeoff) 之空頻碼。於第二個子計畫中我們完成對以低密度對偶碼串接阿拉姆提碼之性能驗證，然後以此碼為基礎設計出具低複雜度的降低 MIMO-OFDM 的峰均比之新方法。於第三個子計畫中我們以髒紙編碼觀念設計出增加功率放大器線性範圍之方法。此外也設計出降低單載波 MIMO 峰均比之方法。

Abstract

In this report, we present the fruitful results of the three subprojects. For the first subproject, we have an optimal construction of space-frequency codes based on the pairwise error probability (PEP) criterion. We also have a systematic construction of SIMO-OFDM space-frequency codes meeting the diversity-multiplexing gain trade-off based on the codeword error probability point of view. For the second subproject, we have completed the investigation of an efficient MIMO-OFDM system, which is constructed by the concatenation of LDPC coding and Alamouti coding. Then, we propose a low-complexity PAPR reduction technique for the investigated space frequency code. For the third subproject, we use Dirty Paper Coding (DPC) to extend the linear range of power amplifiers (PAs) for the single input single output (SISO) single carrier case. We develop a method that can reduce the PAPR of MIMO single carrier systems without sacrificing the optimality of diversity-multiplexing gain tradeoff .

Contents

1	Introduction	7
2	Optimal coding and Modulation Designs for the Fourth Generation Mobile Communication Systems under various MIMO-OFDM Channels	11
2.1	Constructions of Asymptotically Optimal Space-Frequency Codes for MIMO-OFDM Systems Based on PEP Criteria	13
2.1.1	Constructions of Linearly Transformed MRD Codes	21
2.2	Optimal Constructions of SIMO-OFDM Space-Frequency Codes Based on Diversity-Multiplexing Gain Tradeoff (DMT)	25
2.2.1	Outage Probability of the SIMO-OFDM Systems	27
2.2.2	DMT and Optimal Code Constructions	28
3	MIMO OFDM Systems with Low PAPR and Error Rates	33
3.1	The Space-Frequency Code Under Investigation	34
3.2	Simulation Results	37
3.3	PAPR Reduction	41

3.4	CARI Scheme	42
3.5	Time-Domain Circular Shift Scheme	45
3.5.1	Time-Domain Circular Shift Scheme	45
3.6	Simulation Results	47
3.6.1	CCDF Performance	47
3.6.2	BER Performance	49
4	Extending The Linear RAnge of Power Amplifiers with Precoding	54
4.1	Extending the Linear Range of Power Amplifiers with DPC	55
4.2	PAPR Reduction of Space-Time Codes That Achieve D-MG Tradeoff	59
4.2.1	Approximate Cubic Shaping for D-MG Tradeoff Codes	60
4.2.2	Numerical Results	64
5	Conclusions and Remarks	66

List of Tables

3.1	Numeric power delay profile of six paths and two paths.	38
3.2	Four operations of each subblock.	43
3.3	Comparison of information bit S and the number of IFFT needed ξ . .	48
4.1	Without shaping.	64
4.2	After shaping.	65

List of Figures

2.1	(a) Rate-diversity tradeoff for the (4×256) space-frequency codes based upon (2.11) and (b) based upon (2.12).	20
2.2	The number fields K required for constructing the proposed $(1 \times Q)$ SF code. The map id is the identity automorphism.	29
3.1	A block diagram of the space-frequency code under investigation. . .	34
3.2	Power delay profile of six paths and two paths.	37
3.3	BER of considered SF codes, $N_t = N_r = 2$, QPSK modulation	39
3.4	BER of considered SF codes, $N_t = N_r = 2$, 8PSK modulation	40
3.5	BER of considered SF codes, $N_t = 2, N_r = 1$, QPSK modulation . . .	40
3.6	BER of considered SF codes, $N_t = N_r = 1$, 8PSK modulation	41
3.7	Partition of the C_a and C_b	43
3.8	Cross-Antenna Rotation and Inversion (CARI) scheme.	44
3.9	Block diagram of SS-CARI scheme.	45
3.10	Successive Suboptimal Cross-Antenna Rotation and Inversion (SS-CARI) scheme.	45

3.11	Time-domain circular shift (TDCS) scheme.	46
3.12	SS-CARI and TDCS scheme for different value of candidates Q	49
3.13	SS-CARI BER performance for $W = 4$	50
3.14	TDCS BER performance for $Q = 16$	51
3.15	SS-CARI BER performance for $W = 4$ with side information embedded.	52
3.16	TDCS BER performance for $Q = 16$ with side information embedded.	53
4.1	The system model for the proposed precoding scheme.	57
4.2	BER versus SNR for the proposed precoding scheme and systems without precoding with different minimum distances.	58

Chapter 1

Introduction

It is well recognized that MIMO-OFDM (multiple-input multiple output orthogonal frequency division multiplexing) [1] is a promising technique for achieving broadband transmission over possibly frequency selective fading channels. Prof. Hsiao-Feng Francis Lu of Department of Communication Engineering, National Chung-Cheng University, Prof. Hsuan-Jung Su of Graduate Institute of Communication Engineering, and Department of Electrical Engineering, National Taiwan University and I (Mao-Chao Lin, Graduate Institute of Communication Engineering and Department of Electrical Engineering, National Taiwan University) jointly conduct a three-year project beginning August 1 of 2007 for investigating a core issue of MIMO-OFDM, i.e., the coding and modulation of MIMO OFDM. Prof. Hsiao Feng Francis Lu is responsible for the first subproject titled “Optimal Coding and Modulation Designs for the Fourth Generation Mobile Communication systems under various MIMO-OFDM Channels.” Prof. Hsuan-Jung Su is responsible for the third subproject

titled “Extending the Linear Range of Power Amplifiers with Precoding.” I, myself, is responsible for the second subproject titled “PAPR Reduction for the MIMO OFDM Systems.”

In the first year of this research, we have many interesting results which will be detailedly presented in the reports of the respective subprojects and will be briefly summarized in this report of the main project.

For the first subproject, we are concerned with the optimal constructions of space-frequency codes under various MIMO-OFDM channels and two major results will be reported. The first result is an optimal construction of space-frequency codes based on the pairwise error probability (PEP) criterion and will be presented in Chapter 2. This result will be published in *IEEE Transactions on Information Theory*, vol. 53, no. 5, 2007 as a *regular paper*. Specifically, in Chapter 2 we first provide a PEP analysis of the space-frequency codes over MIMO-OFDM channel and then show that there is a tradeoff among the symbol rate, minimal rank distance, and the minimal column distance for the space-frequency codes. Bounds on the tradeoff are given therein. One of the bound is based on the Gilbert-Varshamov argument and is generally considered as the best possible in coding theory. A systematic construction of space-frequency codes whose performance meets this bound in the asymptotic sense is also presented.

While the first result considers the notion of optimality of space-frequency codes from the angle of PEP analysis, the second one focuses more on the codeword error probability point of view. The diversity-multiplexing gain tradeoff (DMT)

proposed by Zheng and Tse [2] has been shown to be a powerful tool in analyzing the performance tradeoff of space-time codes when the channel is modeled as a quasi-static Rayleigh fading channel. On the other hand, there is almost no known results for the MIMO-OFDM channel, which is in fact a more practical channel and has wide applications in wide-band communication standards, especially the most important 4G mobile communication. Here we take a first step by considering the SIMO-OFDM channel and analyze the corresponding DMT. This result is presented in Chapter 2. Again, a systematic construction of SIMO-OFDM space-frequency codes meeting the DMT is also provided in Chapter 2. It should be noted that the proposed DMT-optimal construction can also be applied to all OFDM-based communication schemes and yield the optimal performance.

For the second subproject, we have completed the investigation of an efficient MIMO-OFDM system, which is constructed by the concatenation of LDPC coding and Alamouti coding. By insuring the good error performance of this concatenated SF code, we further investigate the associated PAPR problem. We propose a low-complexity PAPR reduction technique for the investigated SF code, which is a kind of selective mapping technique implemented on the time-domain. Compared to a known PAPR reduction technique for MIMO-OFDM [3] that is a selective mapping technique implemented on the frequency domain, the proposed PAPR reduction technique is more effective in PAPR reduction in case the number of candidates is not large, even though the proposed technique has lower complexity.

For the third subproject, we investigate the idea of using Dirty Paper Coding

(DPC) to extend the linear range of power amplifiers (PAs) for the single input single output (SISO) single carrier case. The idea behind the proposed method is based on the well known information theoretic result on interference cancellation at the transmitter. In the monumental work by Costa [4]. It was proven that if the interference in the channel is known to the transmitter, cancellation of the interference can be done at the transmitter without increasing the transmission power. As a result, the clean channel capacity can be achieved as if the interference does not exist. Since this technique stems from a completely different philosophy than that of the PAPR reduction and the PA linearization methods, the proposed method can be combined with any of these conventional remedies to achieve linear range extension and PAPR reduction at the same time. Additionally, the proposed method can be combined with the cancellation of channel interferences as a unified precoder with small overhead. In addition, we also study the effect of peak to average power ratio (PAPR) constraint on the diversity-multiplexing (DM) tradeoff of multiple input multiple output (MIMO) channel. After this issue is addressed, we develop a method that can reduce the PAPR of MIMO single carrier systems without sacrificing the optimality of DM tradeoff.

Summaries of the first-year research works of the first , the second and the third subprojects are presented in Chapters 2, 3 and 4 respectively. Concluding Remarks are given in Chapter 5.

Chapter 2

Optimal coding and Modulation Designs for the Fourth Generation Mobile Communication Systems under various MIMO-OFDM Channels

In this chapter, brief description of the research work of subproject 1 “Optimal coding and Modulation Designs for the Fourth Generation Mobile Communication Systems under various MIMO-OFDM Channels” is reported. We are concerned with the optimal constructions of space-frequency codes under various MIMO-OFDM channels and two major results will be reported here. The first result is an optimal

construction of space-frequency codes based on the pairwise error probability (PEP) criterion and will be presented in Section 2.1. This result will be published in *IEEE Transactions on Information Theory*, vol. 53, no. 5, 2007 as a *regular paper*. Specifically, in Section 2.1 we first provide a PEP analysis of the space-frequency codes over MIMO-OFDM channel and then show that there is a tradeoff among the symbol rate, minimal rank distance, and the minimal column distance for the space-frequency codes. Bounds on the tradeoff are given therein. One of the bound is based on the Gilbert-Varshamov argument and is generally considered as the best possible in coding theory. A systematic construction of space-frequency codes whose performance meets this bound in the asymptotic sense is also presented.

While the first result considers the notion of optimality of space-frequency codes from the angle of PEP analysis, the second one focuses more on the codeword error probability point of view. The diversity-multiplexing gain tradeoff (DMT) proposed by Zheng and Tse [2] has been shown to be a powerful tool in analyzing the performance tradeoff of space-time codes when the channel is modeled as a quasi-static Rayleigh fading channel. On the other hand, there is almost no known results for the MIMO-OFDM channel, which is in fact a more practical channel and has wide applications in wide-band communication standards, especially the most important 4G mobile communication. Here we take a first step by considering the SIMO-OFDM channel and analyze the corresponding DMT. This result is presented in Section 2.2.1. Again, a systematic construction of SIMO-OFDM space-frequency codes meeting the DMT is also provided in Section 2.2.2. It should be noted that

the proposed DMT-optimal construction can also be applied to all OFDM-based communication schemes and yield the optimal performance.

2.1 Constructions of Asymptotically Optimal Space-Frequency Codes for MIMO-OFDM Systems Based on PEP Criteria

Consider a MIMO-OFDM coded system with n_t transmit and n_r receive antennas. Each OFDM symbol consists of Q subcarriers. Channel coding schemes dedicated to such system are commonly referred to as $(n_t \times Q)$ *space-frequency* (SF) codes [5, 6]. An $(n_t \times Q)$ SF code \mathcal{S} is a set of $(n_t \times Q)$ matrices whose entries are drawn from some signal constellation \mathcal{A} . Code matrices S of the SF code \mathcal{S} are assumed to satisfy an average power constraint, namely,

$$\mathbb{E}_{\mathcal{S}} \{ \|S\|_F^2 \} = n_t Q,$$

where $\|\cdot\|_F$ denotes the Frobenius norm of a matrix.

Following [6] we assume that the MIMO channel undergoes frequency selective fading with L multi-paths. We also assume that the channel is fixed within an OFDM symbol period. Thus the channel between the m th transmit and the n th receive antenna can be modeled in the time domain as the following discrete impulse response:

$$h_{n,m}[k] = \sum_{\ell=0}^{L-1} h_{n,m}^{(\ell)} \delta[k - \tau_{\ell}], \quad (2.1)$$

where $h_{n,m}^{(\ell)}$ and τ_ℓ are respectively the channel gain and path delay associated with the ℓ th fading path and $\delta[k]$ denotes the conventional Kronecker delta function. The $h_{n,m}^{(\ell)}$'s are modeled as i.i.d., circularly symmetric complex Gaussian random variables $\mathbb{C}\mathcal{C}(0, \sigma_\ell^2)$. Without loss of generality, we will assume $\sigma_\ell > 0$ for all ℓ . Furthermore, powers of the L paths are normalized such that

$$\sum_{\ell=0}^{L-1} \sigma_\ell^2 = 1. \quad (2.2)$$

To transmit the code matrix $S \in \mathcal{S}$, the OFDM modulator first applies to each row of S a Q -point inverse fast Fourier transform (IFFT). After attaching to each row of the resultant matrix a cyclic prefix of length no less than L , the m th row of the augmented matrix is transmitted via the m th transmit antenna. At the receiver end, after removing the cyclic prefix from the time-domain received signal matrix, and applying FFT to the rows of the resultant matrix, it can be shown that the received signal matrix Y in the frequency domain is [6]

$$Y = \sqrt{\frac{\text{SNR}}{n_t}} \underbrace{[H_0 \ H_1 \ \cdots \ H_{L-1}]}_{\tilde{H}} \underbrace{\begin{bmatrix} \sigma_0 S \\ \sigma_1 S U^{\tau_1} \\ \vdots \\ \sigma_{L-1} S U^{\tau_{L-1}} \end{bmatrix}}_{:=\tilde{S}} + W \quad (2.3)$$

where

$$H_\ell := \frac{1}{\sigma_\ell} \begin{bmatrix} h_{1,1}^{(\ell)} & h_{1,2}^{(\ell)} & \cdots & h_{1,n_t}^{(\ell)} \\ h_{2,1}^{(\ell)} & h_{2,2}^{(\ell)} & \cdots & h_{2,n_t}^{(\ell)} \\ \vdots & \vdots & \ddots & \vdots \\ h_{n_r,1}^{(\ell)} & h_{n_r,2}^{(\ell)} & \cdots & h_{n_r,n_t}^{(\ell)} \end{bmatrix},$$

$$U := \begin{bmatrix} 1 & & & \\ & e^{-i2\pi\Delta f} & & \\ & & \ddots & \\ & & & e^{-i2\pi(Q-1)\Delta f} \end{bmatrix},$$

and W is the $(n_r \times Q)$ noise matrix, of which $\Delta f = 1/T$ is the subcarrier separation and T is the OFDM symbol period. Entries of W are assumed to be i.i.d., circularly symmetric, complex Gaussian random variables $CN(0, 1)$. Matrix \tilde{H} is termed the *equivalent channel matrix* of size $(n_r \times n_t L)$ and \tilde{S} is termed the *equivalent transmitted signal matrix* of size $(n_t L \times Q)$.

Assuming that the channel state information $\{h_{n,m}^{(\ell)}\}$ is completely known to the receiver, following the analysis in [7, 8, 5], the maximal pairwise error probability is upper bounded ¹ by

$$\text{PEP}_{\max} := \max_{S \neq S' \in \mathcal{S}} \left[\prod_{i=1}^{\nu} \left(1 + \frac{\text{SNR}}{4n_t} \lambda_i \right) \right]^{-n_r}, \quad (2.4)$$

where ν is the rank of the difference matrix $\Delta\tilde{S} = \tilde{S} - \tilde{S}'$ and λ_i are the nonzero eigenvalues of matrix $\Delta\tilde{S}\Delta\tilde{S}^\dagger$. At large SNR regime, the value of PEP_{\max} approxi-

¹A close-form expression for PEP can be found for example, in [8].

mates

$$\text{PEP}_{\max} \approx \text{SNR}^{-dn_r}, \quad (2.5)$$

where

$$d := \min_{S \neq S' \in \mathcal{S}} \text{rank}(\tilde{S} - \tilde{S}'), \quad (2.6)$$

is termed *transmit diversity gain* and the exponent dn_r is commonly referred to as the *diversity gain*.

Given an $(n_t \times Q)$ SF code \mathcal{S} , the transmit diversity gain of \mathcal{S} is bounded by [5]

$$d_r \leq d \leq \min\{Ld_r, d_c\}, \quad (2.7)$$

where

$$d_r := \min_{S \neq S' \in \mathcal{S}} \text{rank}(S - S') \quad (2.8)$$

is the conventional minimum rank distance of \mathcal{S} . d_c is the minimum column distance of \mathcal{S} defined by

$$d_c := \min_{S \neq S' \in \mathcal{S}} w_c(S - S'), \quad (2.9)$$

where the notion of column weight $w_c(\cdot)$ is defined as $w_c(A) = q$ if there are q nonzero columns in the matrix A . The lower bound appearing in (2.7) corresponds to the case when $L = 1$, i.e., the flat fading case.

In addition to the rank distance criterion, the significance of the column distance for designing SF codes was recognized in [5, 9, 10, 11]. A 16-state ST trellis code with $d_c = 3$ for $n_t = 2$ was reported in [5]. With slightly modifying this 16-state code, two 256-state ST trellis codes were proposed in [10], having respectively $d_c = 3$ and $d_c = 6$. It was shown by simulation that the latter achieves about a 4dB

performance gain better than the former due to the increase on minimum column distance d_c . It is therefore seen [10] that the minimum column distance d_c of SF codes plays an important role in the MIMO-OFDM system over frequency-selective fading. Following this perspective, a concatenated Reed-Solomon (RS) and ST trellis code is also reported in [10] to further improve the code performance by using the RS code as the outer code. Likewise, a group space-time-frequency (GSTF) code that is similar to the ST block cyclic codes introduced by the same authors earlier in [12] is presented in [11].

In general without proper channel feedback, the power-delay profile $\{\sigma_\ell, \tau_\ell : \ell = 0, 1, \dots, (L-1)\}$ cannot be known to the transmitter. Furthermore, the exact value of transmit diversity gain d would depend not only on the number of multi-path present in the channel, but also on the specific power-delay profile as shown in (2.6). Therefore, for the sake of having a universal code design criterion, (2.7) suggests that we shall jointly maximize the minimum rank distance d_r and the minimum column distance d_c of code \mathcal{S} . Almost all the earlier works [5, 9, 10, 11] on the constructions of SF codes seek to get larger values of d_c without compromising the minimum rank distance d_r . Clearly, the maximal possible d_r cannot exceed the number of transmit antennas n_t , and the value of d_c is upper bounded by the number of subcarriers Q . Furthermore, conventional wisdom would suggest that the larger the values of d_r and d_c , the smaller the size of the SF code \mathcal{S} . The large values of d_r and d_c would inevitably place more restrictions on the content of \mathcal{S} , hence would reduce the rate of \mathcal{S} . Conversely, SF codes of large rate would have too many codewords to have

good minimum distances d_r and d_c .

To explicitly characterize the relation among these three quantities, let R_s denote the symbol rate of the $(n_t \times Q)$ SF code \mathcal{S} given by

$$R_s := \log_{|\mathcal{A}|} |\mathcal{S}|, \quad (2.10)$$

where \mathcal{A} is the transmitted signal constellation in the frequency domain, e.g. PAM, QAM, PSK etc. Thus, SF codes with symbol rate R_s transmit on the average, R_s constellation symbols, or equivalently $R_b = R_s \log_2 |\mathcal{A}|$ information bits, per OFDM symbol period. Analogous to the rate-diversity tradeoff provided in [13] for quasi-static Rayleigh fading channels, there is also a rate-diversity tradeoff among the symbol rate R_s , the maximal achievable minimum rank distance d_r , and the maximal achievable minimum column distance d_c for the MIMO-OFDM frequency selective fading channels. The following proposition provides an upper bound on such tradeoff by using the Singleton bound argument.

Proposition 1 *For any $(n_t \times Q)$ SF code \mathcal{S} with symbol rate R_s , minimum rank distance d_r , and minimum column distance d_c , we have the following inequality:*

$$R_s \leq \min\{Q(n_t - d_r + 1), n_t(Q - d_c + 1)\}. \quad (2.11)$$

■

While the upper bound (2.11) on the tradeoff is valid for all SF codes, conventional coding theory results also suggest that the Singleton upper bound resulting from the d_c constraint might not be achievable. In order to faithfully reflect the

tradeoff in the practical situation, the following result shows the existence of codes that is generally regarded as the best possible in coding theory.

Theorem 2 (Gilbert-Varshamov bound[14]) *There exists a linear block code with length Q , code rate R , and minimum Hamming distance d_c over \mathbb{F}_q provided if*

$$\sum_{j=1}^{d_c-2} \binom{Q-1}{j} (q-1)^j \leq q^{Q(1-R)}. \quad (2.12)$$

Moreover, as the block length Q tends to infinity, we have that

$$\delta = \lim_{Q \rightarrow \infty} \frac{d_c}{Q} \geq h_q^{-1}(1-R), \quad (2.13)$$

where $h_q^{-1}(x)$ is the inverse of the entropy function given by

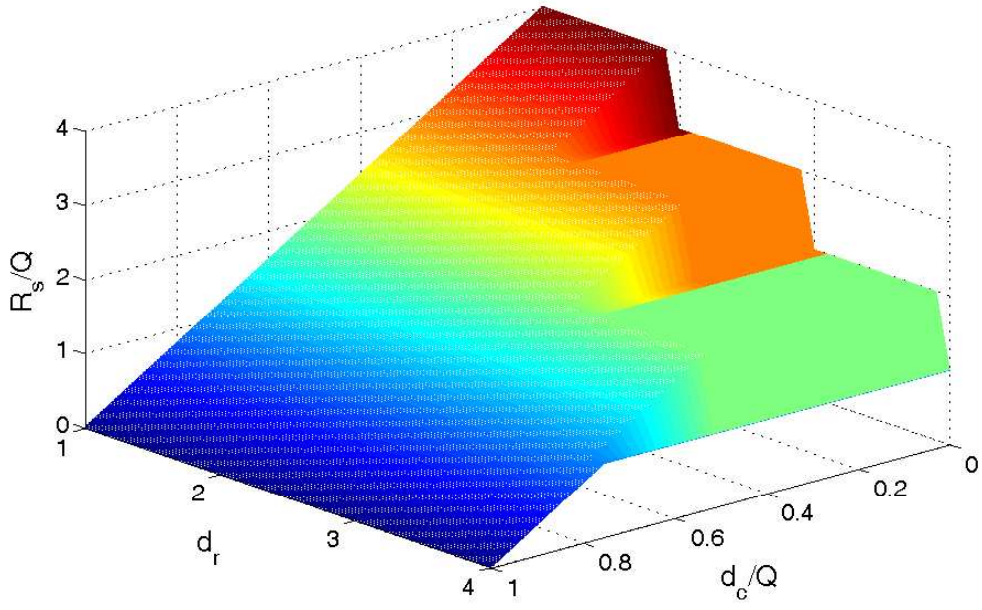
$$h_q(x) = x \log_q(q-1) - x \log_q x - (1-x) \log_q(1-x). \quad (2.14)$$

■

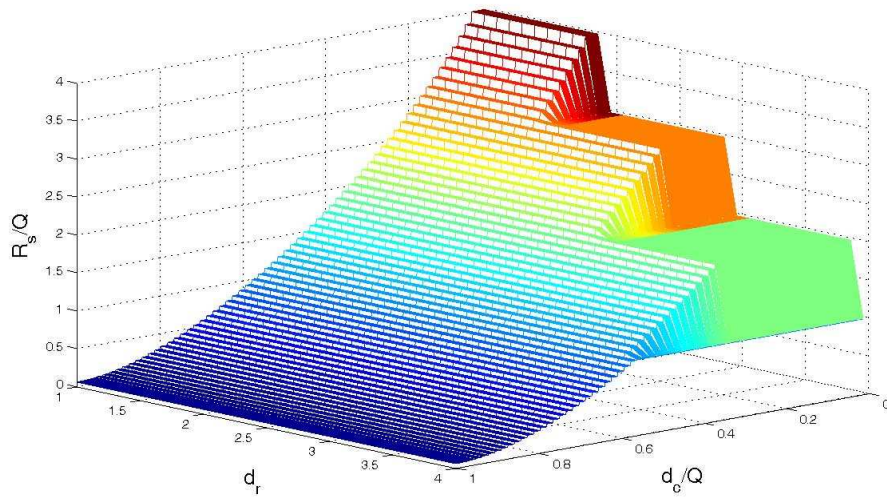
Remark 1 *In general it is very difficult to have codes performed better than the G-V bound except when the underlying field is very large [15], compared to the code length Q . Thus, based on the well-established results in error correcting codes [14], we shall speculate that there might exist $(n_t \times Q)$ binary SF codes having rate R_s , minimum rank distance d_r , and minimum column distance d_c such that*

1. the pair (R_s, d_r) satisfies the first constraint of (2.11), and at the same time,
2. the pair $\left(R = \frac{R_s}{n_t Q}, d_c\right)$ achieves the G-V bound in (2.12).

■



(a)



(b)

Figure 2.1: (a) Rate-diversity tradeoff for the (4×256) space-frequency codes based upon (2.11) and (b) based upon (2.12).

Example 1 *In this example we consider the rate-diversity tradeoffs for the (4×256) space-frequency code. That is, we have $n_t = 4$ and $Q = 256$. The corresponding tradeoff is shown in Fig. 2.1. ■*

Surprisingly, the above speculation turns out to be true in general and an explicit, systematic construction of SF codes meeting both the above conditions will be given in the next section.

2.1.1 Constructions of Linearly Transformed MRD Codes

Given the desired symbol rate R_s , in this section we will present a construction of $(n_t \times Q)$ SF codes that achieves the maximal possible rank distance d_r and at the same time, has the minimum column distance d_c meeting the G-V bound (2.13) in the asymptotic sense. For the sake of brevity, here we will only focus on the construction of binary codes, i.e., $\mathcal{A} = \mathbb{F}_2$, while the construction itself can be extended to cater to the non-binary cases.

The construction calls for the rank- d_r $(n_t \times Q)$ binary MRD codes constructed in [16, 13]. Recall that for every d_r , n_t and Q with $d_r \leq n_t \leq Q$, in [16, 13] there is a systematic way of constructing the rank- d_r $(n_t \times Q)$ binary MRD codes. The resultant MRD codes will meet the Singleton bound on the rate, i.e., have symbol rate $R_s = Q(n_t - d_r + 1)$. However, it can be verified that the minimum column distance d_c of the MRD codes equals d_r in many cases, which is far from being optimal in terms of G-V bound (2.12). Thus, below we consider a linear transformation technique to further improve its minimum column distance.

Let \mathcal{S} be a rank- d_r ($n_t \times Q$) binary MRD code and consider the following code

$$\mathcal{SG} = \{SG : S \in \mathcal{S}\},$$

where $G \in GL_Q(\mathbb{F}_2)$ is some $(Q \times Q)$ nonsingular binary matrix and where $GL_Q(\mathbb{F}_2)$ is the general linear group consisting of all $(Q \times Q)$ nonsingular binary matrices. SF codes obtained in this fashion will be termed *linearly transformed-MRD* (LT-MRD) codes in this report. It is straightforward to see that the LT-MRD code \mathcal{SG} has same rank distance d_r as \mathcal{S} for any $G \in GL_Q(\mathbb{F}_2)$. While multiplying \mathcal{S} on the right by G would not affect the rank distance d_r , the minimum column distance of \mathcal{SG} can vary with different G s, as for any $S \neq S' \in \mathcal{S}$, we have $w_c(S - S') \neq w_c(SG - S'G)$ in general.

To see the minimum column distance of the LT-MRD code \mathcal{SG} , here we consider the code ensembles $\{SG : G \in GL_Q(\mathbb{F}_2)\}$ for all $(Q \times Q)$ nonsingular binary matrices G . Arguing probabilistically, we shall define the minimum column distance d_c of the ensemble code $\{SG\}$ as

$$d_c = \min \left\{ q > 0 : \frac{1}{|\mathcal{S}|} \mathbb{E}_G \left| \{(S, S') \in \mathcal{S}^2 : w_c(SG - S'G) = q\} \right| \geq 1 \right\}, \quad (2.15)$$

meaning that for $d \leq d_c$, there exists a matrix G such that the minimal column distance of code \mathcal{SG} is larger than d . We claim that the minimum column distance d_c of the ensemble code $\{SG\}$ achieves the asymptotic G-V bound. We have the following theorem.

Theorem 3 (Binary LT-MRD Codes) *For $q = 2$, the column weight distribu-*

tion of binary $(n_t \times Q)$ $\mathcal{S}\mathcal{G}$ code is

$$\begin{aligned} W_t &:= \mathbb{E}_G \{S \in \mathcal{S} : w_c(SG) = t\} \\ &= \sum_{k=0}^{n_t} \frac{\binom{Q}{t} A(k, t) B_k(n_t, Q, d_r)}{\prod_{i=0}^{k-1} (2^Q - 2^i)} \end{aligned} \quad (2.16)$$

where

$$A(k, t) = \sum_{i=0}^k (-1)^i \begin{bmatrix} k \\ k-i \end{bmatrix}_2 2^{\binom{i}{2}} (2^{k-i} - 1)^t \quad (2.17)$$

$$B_k(n_t, Q, d_r) := \begin{bmatrix} n_t \\ k \end{bmatrix}_2 \sum_{j=0}^{k-d_r} (-1)^j \begin{bmatrix} k \\ j \end{bmatrix}_2 2^{j(j-1)/2} (2^{Q(k-d_r-j+1)} - 1). \quad (2.18)$$

■

Corollary 4 (Asymptotic LT-MRD Codes) *For any the integer pair (n_t, d_r) with $d_r \leq n_t$ and for any integer $Q \geq n_t$ set $R_s = Q(n_t - d_r + 1)$ and let \mathcal{S}_Q be a rank- d_r $(n_t \times Q)$ binary MRD code of size 2^{R_s} . Let d_c be the minimum column distance of the ensemble code $\{\mathcal{S}_Q G\}$ defined in (2.15); then as $Q \rightarrow \infty$ we have*

$$\delta \geq \lim_{Q \rightarrow \infty} \frac{d_c}{Q} = h_{2^{n_t}}^{-1} \left(\frac{d_r - 1}{n_t} \right), \quad (2.19)$$

where $h_{2^{n_t}}^{-1}(x)$ is the inverse of the entropy function given by (2.14). That is, the ensemble code $\{\mathcal{S}_Q G\}$ achieves the asymptotic G-V bound on the minimum column distance.

■

Example 2 To design a (2×256) LT-MRD code, we begin with the construction of a full rank binary (2×256) MRD code \mathcal{S} , i.e. $n_t = 2$, $Q = 256$, $d_r = 2$, and \mathbb{F}_q with $q = 2$. Such SF code has rate $R_s = Q(n_t - d_r + 1) = 256$ bits/OFDM symbol. But this code performs poorly on the minimal column distance, ending up with $d_c = 2$. However, the Gilbert-Varshamov bound (2.12) asserts that there exist SF codes with

$$d_c = d_{GV}(n_t, Q, R_s, q) = 51 \quad (2.20)$$

Now by the LT-MRD code construction, one can randomly pick $G \in GL_Q(\mathbb{F}_2)$ and Theorem 3 asserts that the resultant code $\mathcal{S}G$ will have minimal column distance d_c with probability

$$\Pr \{d_c \geq 50\} \geq 0.2515,$$

$$\Pr \{d_c \geq 49\} \geq 0.9803,$$

$$\Pr \{d_c \geq 48\} \geq 0.9985,$$

$$\Pr \{d_c \geq 47\} \geq 0.9999,$$

$$\Pr \{d_c \geq 46\} \geq 0.999991806.$$

■

2.2 Optimal Constructions of SIMO-OFDM Space-Frequency Codes Based on Diversity-Multiplexing Gain Tradeoff (DMT)

Recall in Section 2.1 that the sampled impulse response between the transmit and the receive antennas is modeled as a length- n_r discrete-time vector

$$\underline{h}[k] := \sum_{\ell=0}^{L-1} \sigma_{\ell} \underline{h}_{\ell} \delta[k - \tau_{\ell}]. \quad (2.21)$$

where $\underline{h}_{\ell} = [h_{0,0}^{(\ell)}, h_{1,0}^{(\ell)}, \dots, h_{n_r-1,0}^{(\ell)}]^t$ and $h_{n,0}^{(\ell)}$ are i.i.d. zero-mean, complex Gaussian random variables with unit variance. Given the channel impulse response vector $\underline{h}[k]$, it is easy to see that the frequency response at the q th subcarrier is

$$\underline{g}_q := \sum_{\ell=0}^{L-1} \sigma_{\ell} \omega_Q^{q\tau_{\ell}} \underline{h}_{\ell}, \quad (2.22)$$

where $\omega_Q = \exp(i 2\pi/Q)$, $i = \sqrt{-1}$. The $(1 \times Q)$ SF \mathcal{S} is a set of length- Q vectors $\underline{x} = [x_0, \dots, x_{Q-1}]^t$ whose entries x_q are drawn from some signal constellation set. In particular, the code \mathcal{S} is assumed to satisfy the following average power constraint:

$$\mathbb{E}_{\mathcal{S}} \|\underline{x}\|^2 = \frac{1}{|\mathcal{X}|} \sum_{\underline{x} \in \mathcal{S}} \|\underline{x}\|^2 = Q, \quad (2.23)$$

where by $\|\underline{x}\|$ we mean the Frobenius norm of the vector \underline{x} . Given the code vector $\underline{x} \in \mathcal{S}$, the received signal vector \underline{y}_q at the q th subcarrier is given by

$$\underline{y}_q = \sqrt{\text{SNR}} \underline{g}_q x_q + \underline{w}_q, \quad (2.24)$$

where the entries of the vectors \underline{w}_q , $q = 0, 1, \dots, Q-1$, are the additive i.i.d. complex Gaussian noise with zero mean and unit variance.

When the receiver has complete channel state information, but not the transmitter, i.e. only the receiver has the complete knowledge of the frequency response vectors $\{\underline{g}_q\}$ defined in (2.22). As the transmitter has no fore-knowledge of the channel, for the sake of calculating the ergodic channel capacity of this channel, following similar arguments as in [17, 2] it can be shown that at larger SNR regime we can assume without loss of generality that the input \underline{x} are i.i.d. complex Gaussian random vectors with covariance matrix $R_{xx} = I_Q$. Thus the ergodic channel capacity is given by the following theorem. It should be noted that in the above capacity result, the rate loss due to the insertion of cyclic prefix has been neglected.

Theorem 5 *For any SIMO-OFDM system with n_r receive antennas and Q subcarriers and for any frequency selective Rayleigh fading channel with power-delay profile $\{\sigma_\ell^2, \tau_\ell : \ell = 0, 1, \dots, L - 1\}$, $L \leq Q$, the ergodic channel capacity of such system equals*

$$\mathcal{C}(\text{SNR}) = \log \text{SNR} + O(1)$$

at large SNR regime. ■

While the above theorem shows that the ergodic channel capacity for the frequency selective Rayleigh fading channel is same as the one for the flat Rayleigh fading channel [17], their outage capacities can be different. The outage probability of the latter is known [2] to approximate $\text{SNR}^{-n_r(1-r)}$ when the target rate is set at $R = r \log \text{SNR}$ nats/second/Hz. When $n_r = 1$, the outage probability of the SISO-OFDM frequency selective Rayleigh fading channel approximates $\text{SNR}^{-L(1-r)}$,

shown by Gropop and Tse [18]. In the next section we will investigate the outage capacity of the SIMO-OFDM channel.

2.2.1 Outage Probability of the SIMO-OFDM Systems

Recall from [2] that the outage probability $P_{\text{Out}}(r)$ is defined as

$$P_{\text{Out}}(r) = \Pr \left\{ \frac{1}{Q} \sum_{q=0}^{Q-1} \log \left(1 + \text{SNR} \left\| \underline{g}_q \right\|^2 \right) \leq r \log \text{SNR} \right\}, \quad (2.25)$$

where $r \in [0, 1]$ is commonly referred to as the *multiplexing gain* [2]. Literally, $P_{\text{Out}}(r)$ is the probability that the mutual information between \underline{x} and received signal vectors $\{\underline{y}_q, q = 0, \dots, Q-1\}$ is less than or equal to the target rate $R = r \log \text{SNR}$. The outage probability $P_{\text{Out}}(r)$ is said to have an outage exponent $d_{\text{Out}}(r)$ if

$$P_{\text{Out}}(r) \doteq \text{SNR}^{-d_{\text{Out}}(r)}, \quad (2.26)$$

where by \doteq we mean the exponential equality, explicitly defined in [2]. Notions of $\dot{\leq}$ and $\dot{\geq}$ are defined similarly.

To obtain the outage exponent $d_{\text{Out}}(r)$, we first set

$$\alpha_{n,\ell} := -\frac{\log |h_{n,\ell}|^2}{\log \text{SNR}}, \quad (2.27)$$

meaning

$$h_{n,\ell} = \text{SNR}^{-\alpha_{n,\ell}/2} \exp(j\phi_{n,\ell})$$

for some $\phi_{n,\ell} \in [0, 2\pi)$. Then by definition of \underline{g}_q we see

$$\left\| \underline{g}_q \right\|^2 = \sum_{n=0}^{n_r-1} \left| \sum_{\ell=0}^{L-1} \sigma_\ell \omega^{q\tau_\ell} h_{n,\ell} \right|^2 \doteq \max_{n,\ell} \text{SNR}^{-\alpha_{n,\ell}},$$

which is independent of the choices of q . Now after carefully estimating the error exponent of (2.25) we have the following result.

Theorem 6 *For any SIMO-OFDM system with n_r receive antennas and Q subcarriers and for any frequency selective Rayleigh fading channel with power-delay profile $\{\sigma_\ell^2, \tau_\ell : \ell = 0, 1, \dots, L-1\}$, $L \leq Q$, the outage exponent of such system is given by*

$$d_{\text{Out}}(r) = Ln_r(1 - r) \quad (2.28)$$

for $0 \leq r \leq 1$. ■

Comparing to the conventional flat Rayleigh fading channel considered by Zheng and Tse in [2] we see that the frequency selective channel has a higher outage exponent that grows linearly with the number of multipaths present in the channel. When setting $n_r = 1$ the above result reduces to the outage exponent for the SISO-OFDM channel, which also agrees with the result shown by Gropop and Tse in [18]. When $L = Q$, the resultant channel is equivalent to a fast Rayleigh fading channel and Theorem 6 shows that the outage exponent equals $d_{\text{Out}}(r) = Qn_r(1 - r)$, which coincides exactly with results appearing in [2, 19] when they are generalized to the case of fast Rayleigh fading channel.

2.2.2 DMT and Optimal Code Constructions

Having obtained the outage exponent of the SIMO-OFDM frequency-selective Rayleigh fading channel, we now continue to investigate the DMT of such channel. Given the multiplexing gain r , we say the channel has diversity gain $d(r)$ [2] if there exists a

family of SIMO-OFDM coding schemes $\{\mathcal{S}(\text{SNR})\}$, one at each SNR level, such that the error probability achieved by $\mathcal{S}(\text{SNR})$ approximates

$$P_e(\mathcal{S}(\text{SNR})) \doteq \text{SNR}^{-d(r)}. \quad (2.29)$$

The optimal diversity gain $d^*(r)$ is the supremum of $d(r)$ achieved by all possible coding schemes, i.e.

$$d^*(r) = \sup_{\mathcal{S}(\text{SNR})} d(r). \quad (2.30)$$

Even though it is possible to show $d^*(r) = Ln_r(1-r)$ for the SIMO-OFDM channel by use of the random coding arguments as [2], it would be better to have a fixed, systematic SF code achieving this $d^*(r)$. To this end, below we will provide a construction of SIMO-OFDM $(1 \times Q)$ SF codes.

$$\begin{array}{ccc} K & & \text{Gal}(K/\mathbb{Q}(\iota)) = \langle \sigma \rangle \\ \downarrow Q & & \downarrow \\ \mathbb{Q}(\iota) & & \langle \text{id} \rangle \end{array}$$

Figure 2.2: The number fields K required for constructing the proposed $(1 \times Q)$ SF code. The map id is the identity automorphism.

Let K be a number field over $\mathbb{Q}(\iota)$ as shown in Fig. 2.2. The number field K is a cyclic Galois extension of $\mathbb{Q}(\iota)$ with degree of extension equal to Q , the number of subcarriers in an OFDM symbol. Such a field K can be explicitly constructed by using algorithms given in [19, 20].

Let σ be a generator of the cyclic Galois group $\text{Gal}(K/\mathbb{Q}(\iota))$ and let $\mathcal{B} = \{e_1, e_2, \dots, e_Q\}$ be an integral basis for K over $\mathbb{Q}(\iota)$; then we propose the following

(1 × Q) SF code

$$\mathcal{S} = \left\{ X = [x, \sigma(x), \dots, \sigma^{Q-1}(x)], x = \sum_{i=1}^Q a_i e_i, a_i \in \mathcal{A}(\text{SNR}) \right\}, \quad (2.31)$$

where $\mathcal{A}(\text{SNR})$ is a set of QAM constellation points of size SNR^r . $\mathcal{A}(\text{SNR})$ is termed *base alphabets* in [19].

Proposition 7 *The proposed (1 × Q) SF code \mathcal{S} satisfies the following generalized non-vanishing determinant property: for every $X \neq X' \in \mathcal{S}$, $X = [x_1, x_2, \dots, x_Q]$ and $X' = [x'_1, x'_2, \dots, x'_Q]$, the following holds*

$$\left| \prod_{q=1}^Q (x_q - x'_q) \right| = N(x_1 - x'_1) \geq 1, \quad (2.32)$$

where $N(x)$ is the algebraic norm of x over $K/\mathbb{Q}(\iota)$. ■

There is also a power-scaling parameter θ associated with code \mathcal{S} for ensuring the power constraint criterion for SF codes. The parameter θ is chosen such that

$$\mathbb{E}_{\underline{x}} \|\theta \underline{x}\|^2 \doteq \text{SNR}.$$

Thus we shall set

$$\theta^2 \doteq \text{SNR}^{1-r}$$

and given $\underline{x} \in \mathcal{S}$, the received signal vector at the q th subcarrier is given by

$$\underline{y}_q = \theta x_q \underline{g}_q + \underline{w}_q,$$

where \underline{g}_q and \underline{w}_q are defined as before. Finally we have the following result.

Theorem 8 Let $\mathcal{A}(\text{SNR})$ be a base-alphabet of size SNR^r , where r is the desired value of multiplexing gain, $0 \leq r \leq 1$. Then at large SNR regime, the codeword error probability of the proposed $(1 \times Q)$ SF code \mathcal{S} is upper bounded by

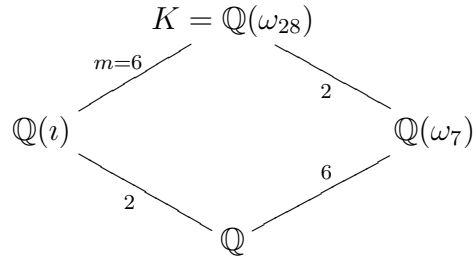
$$P_e(\text{SNR}) \leq \text{SNR}^{-d^*(r)}, \quad (2.33)$$

where

$$d^*(r) = Ln_r(1 - r), \quad (2.34)$$

when the SIMO-OFDM channel is modeled as in (2.21). That is, the code \mathcal{S} is optimal with respect to the DMT defined in (2.28). \blacksquare

Example 3 In this example we will attempt to construct the proposed SF code \mathcal{S} with $Q = 6$. By using classical algebraic number theory, it can be shown that $K = \mathbb{Q}(\omega_{28})$ is a cyclic Galois extension over $\mathbb{Q}(i)$ with degree of extension equal to 6, where by ω_ℓ we mean a complex, primitive ℓ th complex root of unity. We have the following diagram in mind.



As $i = \sqrt{-1} = \omega_{28}^7$, it can be shown that

$$\mathcal{B} = \{\omega_{28}^i : i = 0, \dots, 5\}$$

is an integral basis for K over $\mathbb{Q}(i)$. The Galois group of K over $\mathbb{Q}(i)$ is generated

by the automorphism

$$\sigma : \omega_{28} \mapsto \omega_{28}^5, \quad (2.35)$$

hence

$$\text{Gal}(K/\mathbb{Q}(\iota)) = \langle \sigma \rangle = \{\sigma_1, \sigma_5, \sigma_{25}, \sigma_{13}, \sigma_9, \sigma_{17}\} \cong \mathbb{Z}_6, \quad (2.36)$$

where by σ_i we mean the automorphism

$$\sigma_i : \omega_{28} \mapsto \omega_{28}^i. \quad (2.37)$$

The resultant coding scheme \mathcal{S} is given by

$$\mathcal{S} = \left\{ \left(\sum_{i=0}^5 a_i \omega_{28}^i, \sum_{i=0}^5 a_i \omega_{28}^{5i}, \sum_{i=0}^5 a_i \omega_{28}^{25i}, \sum_{i=0}^5 a_i \omega_{28}^{13i}, \sum_{i=0}^5 a_i \omega_{28}^{9i}, \sum_{i=0}^5 a_i \omega_{28}^{17i} \right) : a_i \in \mathcal{A}(\text{SNR}) \right\} \quad (2.38)$$

for some base-alphabet $\mathcal{A}(\text{SNR}) \subset \mathbb{Z}[\iota]$ having size

$$|\mathcal{A}(\text{SNR})| \doteq \text{SNR}^r$$

with $0 \leq r \leq 1$. It is relatively easy to verify that

$$\prod_{j=0}^5 \left(\sum_{i=0}^5 a_i \omega_{28}^{i \cdot 5^j} \right) = N_{K/\mathbb{Q}(\iota)} \left(\sum_{i=0}^5 a_i \omega_{28}^i \right)$$

lies in $\mathbb{Z}[\iota]$ for all $a_i \in \mathbb{Z}[\iota]$ as claimed by Proposition 7. Following from Theorem 8,

the codeword error performance of \mathcal{S} at high SNR regime is on the order of

$$P_e \doteq \text{SNR}^{-d^*(r)}, \quad (2.39)$$

where the maximal achievable diversity gain $d^*(r)$ is in this case given by

$$d^*(r) = Ln_r(1-r) \quad (2.40)$$

for $0 \leq r \leq 1$ and for any $L \leq 6$. ■

Chapter 3

MIMO OFDM Systems with Low PAPR and Error Rates

In this chapter, the research work about subproject 2 regarding PAPR reduction for MIMO OFDM is briefly reported. As indicated in the last chapter, we are aware that to achieve good error performance of a space-frequency code, we need to maximize γ , the rank of $D(C, \hat{C})$, which is determined by $\hat{\gamma}$ and LN_t , where $\hat{\gamma}$ is the column distance of the codeword difference matrix $C - \hat{C}$ and L is the number of multiple delayed paths. In this chapter, we investigate a space-frequency code with $N_t = 2$, which is the concatenation of a binary LDPC code, signal mapper and the Alamouti space-time code. The reason for using this concatenation is that (i) the binary LDPC code has large binary Hamming distance which can still yield a significant amount of column distance; (ii) the full rank characteristics of Alamouti space-time coding will enhance the column distance of the concatenated coding.

Then, we propose a new PAPR reduction scheme for this space-frequency code.

3.1 The Space-Frequency Code Under Investigation

We now investigate a construction of space-frequency code called the LDPC Coded Alamouti Scheme for MIMO OFDM.

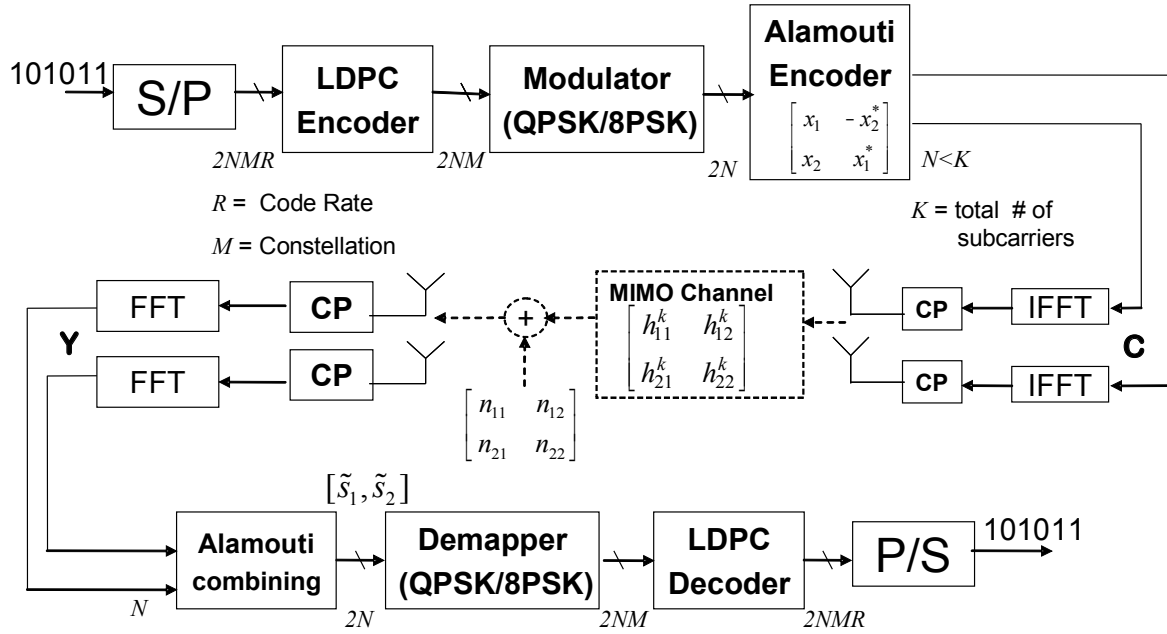


Figure 3.1: A block diagram of the space-frequency code under investigation.

The transmitter and receiver structure of an LDPC coded Alamouti Scheme for MIMO OFDM system is illustrated in Fig.(3.1). We assume that the receiver has perfect channel state information (CSI).

In Fig.(3.1), the $2NMR$ information bits are first encoded by a rate R LDPC encoder into $2NM$ coded bits and then the binary LDPC coded bits are modulated into

$2N$ 2^M PSK¹ symbols. We split these $2N$ symbols into 2 streams, and each stream has N symbols. The N symbols of each stream are transmitted from one transmit antenna which has K subcarrier over an OFDM slot. Usually, we set $N < K$ in order to reserve subcarriers for side information (SI) or some other purposes. We have two streams denoted C_a and C_b which will be transmitted through two transmit antennas respectively. The Alamouti encoder converts these two streams into a space frequency codeword represented by $[C_1, C_2]$, where C_1 and C_2 are described as

$$C_1 = \begin{bmatrix} C_a \\ C_b \end{bmatrix} = \begin{bmatrix} c_1(0) & \dots & c_1(N-1) & c_1(N) & \left| & c_1(N+1) & \dots & c_1(K) \right. \\ c_2(0) & \dots & c_2(N-1) & c_2(N) & \left| & c_2(N+1) & \dots & c_2(K) \right. \end{bmatrix} \quad (3.1)$$

$$C_2 = \begin{bmatrix} -C_b^* \\ C_a^* \end{bmatrix} = \begin{bmatrix} -c_2^*(0) & \dots & -c_2^*(N-1) & -c_2^*(N) & \left| & -c_2^*(N+1) & \dots & -c_2^*(K) \right. \\ c_1^*(0) & \dots & c_1^*(N-1) & c_1^*(N) & \left| & c_1^*(N+1) & \dots & c_1^*(K) \right. \end{bmatrix} \quad (3.2)$$

each $c_i(j)$ is an 2^M PSK symbol, and $c_1(N+1) = \dots = c_1(K) = c_2(N+1) = \dots = c_2(K) = 0$. The symbols represented by C_1 is transmitted in the first OFDM time slot and the symbols represented C_2 is transmitted in the following OFDM time slot. The transmitter applies an K -point IFFT to each row of the matrix C_i and then appends a cyclic prefix (CP), which is then used for transmission.

It is assumed that the fading process remains static during two consecutive OFDM time slots and the fading at every two consecutive OFDM time slots is independent of any other two consecutive OFDM time slots.

At the receiver, we have receives signals from two receive antennas. After

¹For example, $M = 2$ for QPSK, $M = 3$ for 8PSK.

matched filtering and sampling, the FFT is applied to the discrete-time signal to obtain

$$\begin{aligned} Y_1 &= \begin{bmatrix} y_1^1(0) & y_1^1(1) & \dots & y_1^1(K) \\ y_2^1(0) & y_2^1(1) & \dots & y_2^1(K) \end{bmatrix} \\ Y_2 &= \begin{bmatrix} y_1^2(0) & y_1^2(1) & \dots & y_1^2(K) \\ y_2^2(0) & y_2^2(1) & \dots & y_2^2(K) \end{bmatrix} \end{aligned} \quad (3.3)$$

where y_k^i denotes the received signal at the k th subcarriers for i th OFDM time slot. The decoding consists two stages, i.e., the *soft* Alamouti combing and the *soft* LDPC decoder and the so-called extrinsic information passed from first stage to second.

For the first stage of Alamouti combing, Alamouti decoder takes $y_1^1(k)$, $y_2^1(k)$, $y_1^2(k)$ and $y_2^2(k)$ as input, which can be written as

$$\begin{bmatrix} r_{11} & r_{12} \\ r_{21} & r_{22} \end{bmatrix} = \begin{bmatrix} y_1^1(k) & y_1^2(k) \\ y_2^1(k) & y_2^2(k) \end{bmatrix} \quad (3.4)$$

and Alamouti soft decoding can be obtained as the demapper shown in [21]. For each k , there is a pair of symbols $(\tilde{s}_1, \tilde{s}_2)$. For either s_1 or s_2 , there are M associated LLR values. Each LLR value corresponds to an LDPC coded bit. After LDPC decoding, we obtain $2NM$ hard value (1 or 0) for coded bits. Then, $2NMR$ information bits are detected. The LDPC decoding can produce soft output, which can be fed back to the demapper of Alamouti coding for outer iterations (other than the inner iterations inside the LDPC decoding operation). Simulation shows that such outer iterations will be significantly reduce the BER. Hence, in the rest of this report, we only consider the decoding without outer iterations.

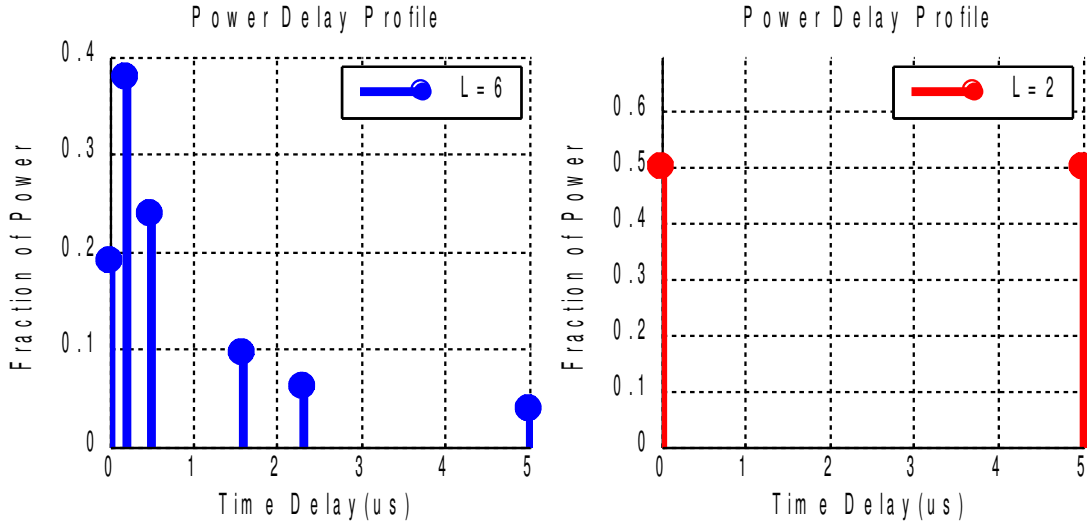


Figure 3.2: Power delay profile of six paths and two paths.

3.2 Simulation Results

In this section, we provide computer simulation results to examine the performance of the LDPC-coded Alamouti scheme. The characteristics of the fading channels are described in Section 2.1. In the following simulations, the available bandwidth is 1MHz and the number of subcarriers is $K = 256$. Thus, the OFDM word duration is $T = 256\mu s$ without the cyclic prefix. We set the length of cyclic prefix to $5\mu s$ to combat the effect of inter-symbol-interference, since the delay is no more than $5\mu s$.

We simulated the space frequency codes with different power delay profiles: (i) a two-ray equal power delay profile and (ii) COST207[22] typical urban six-ray power delay profile. The subcarrier path gains are generated independently for different transmit and receive antennas. The power delay profile of the channel is shown in Fig.(3.2) and Table(3.1). All the LDPC codes used in simulation are regular LDPC codes with column weight $w_c = 3$ in the parity-check matrix and with

Six paths			Two paths		
Delay (us)	Fractional Power	Doppler Category	Delay (us)	Fractional Power	Doppler Category
0.0	0.189	CLASS	0.0	0.500	CLASS
0.2	0.379	CLASS	5.0	0.500	CLASS
0.5	0.239	CLASS			
1.6	0.095	GAUS1			
2.3	0.061	GAUS1			
5.0	0.037	GAUS1			

Table 3.1: Numeric power delay profile of six paths and two paths.

appropriate block lengths and code rates. The modulation under consideration are QPSK or 8PSK constellation respectively. Simulation results are shown in terms of the information bit-error rate (BER) versus E_b/N_0 . The simulation MIMO system has $K = 256$ subcarriers. The LDPC has code rate $R = 0.5$ or 0.667 . The iterations of LDPC codes is 30.

In order to span LDPC coded bits in an OFDM word, the LDPC code length varies with modulation. That is, the LDPC code lengths are 1008 and 1512 with respect to QPSK and 8PSK respectively. Both cases have the same number of modulation symbols, which is $1008/2 = 1512/3 = 504$. The 504 symbols are transmitted by two transmit antennas. Hence, there are 252 modulated symbols to be transmitted by each antenna. Thus, 252 of the 256 subcarriers will be used to represent the 252 symbols, while 4 of the 256 subcarriers are free subcarriers which can be used

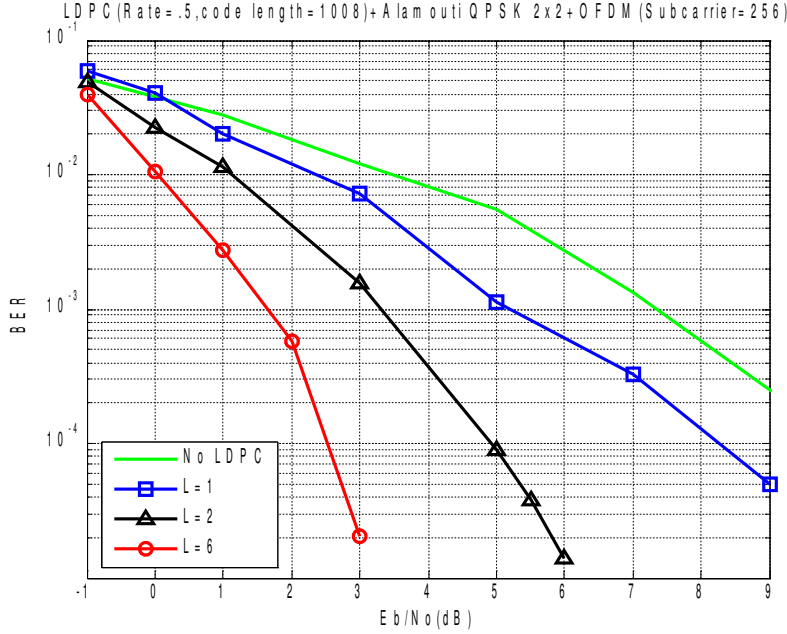


Figure 3.3: BER of considered SF codes, $N_t = N_r = 2$, QPSK modulation

to carry side information or some other purpose. When the LDPC decoder receive (Y_1, Y_2) , an LDPC codeword can be completely decoded.

Fig.(3.3), Fig.(3.4), Fig.(3.5) and Fig.(3.6) depict the performances of the considered space-frequency (SF) codes under the condition of various power delay profiles and various modulation methods. We use the BPSK modulation for the case of not using LDPC and QPSK for the case of using LDPC codes in Fig.(3.3) and Fig.(3.5). Also, we use the QPSK modulation for the case of not using LDPC and 8PSK for the case of using LDPC codes in Fig.(3.4) and Fig.(3.6). Thus, the transmission rate of both cases are the same. Clearly, the performance of the SF codes *without* LDPC²

²The performance of the case without LDPC is independent of the condition of the existence or nonexistence of delay paths.

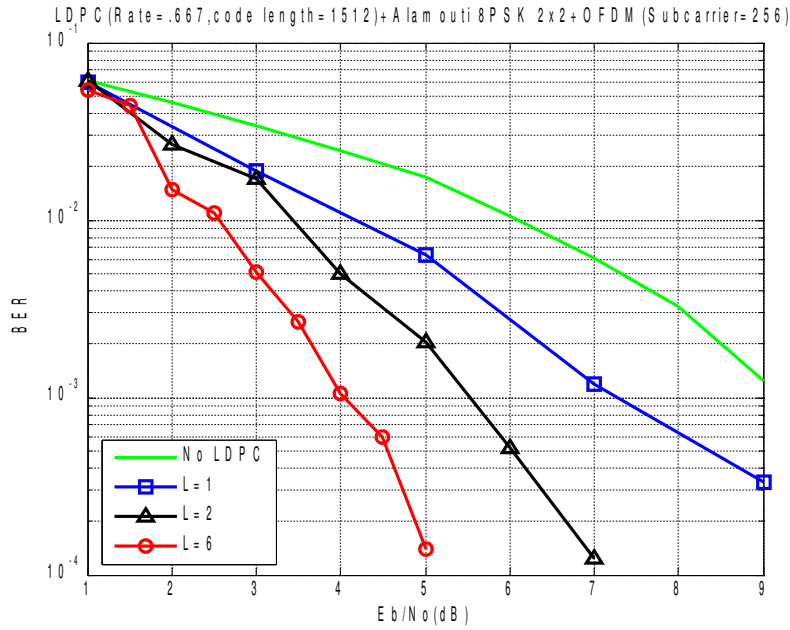


Figure 3.4: BER of considered SF codes, $N_t = N_r = 2$, 8PSK modulation

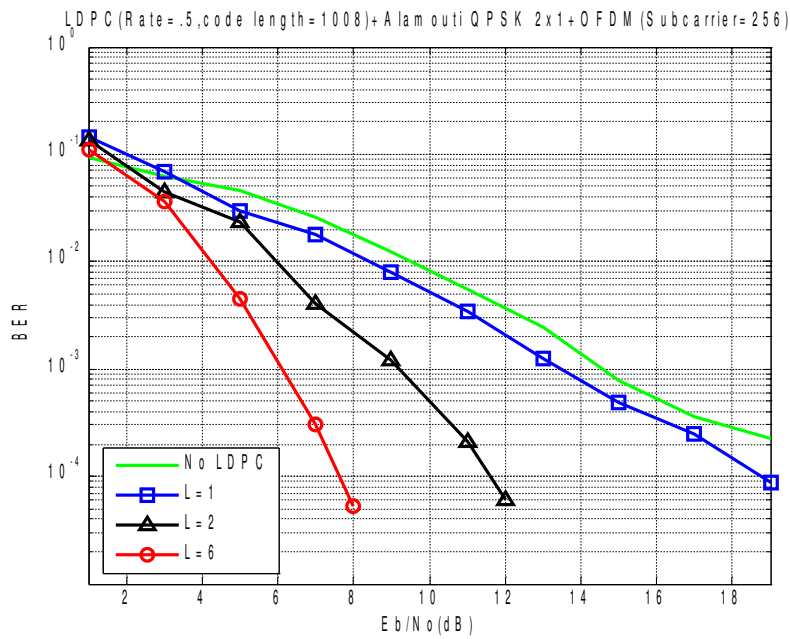


Figure 3.5: BER of considered SF codes, $N_t = 2, N_r = 1$, QPSK modulation

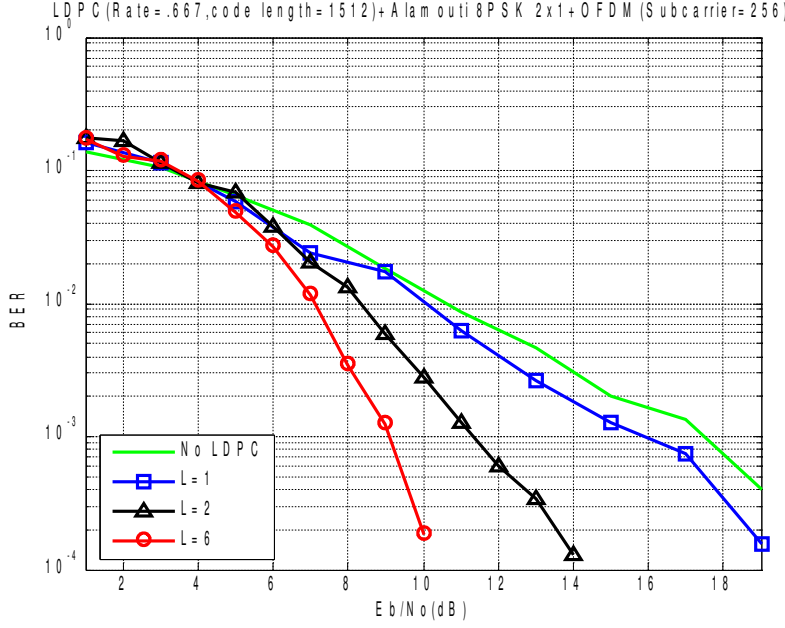


Figure 3.6: BER of considered SF codes, $N_t = N_r = 1$, 8PSK modulation codes, i.e., pure Alamouti coding is much worse than the case of using LDPC codes.

3.3 PAPR Reduction

Consider MIMO OFDM systems with N_t transmit antennas and N_r receive antennas. Denote $PAPR_p$ as the PAPR of the p th transmit antenna. Then for multiple transmit antennas, the PAPR is defined in Definition 1.

DEFINITION 1 *The PAPR of the MIMO OFDM symbol in discrete-time signals is as below*

$$\overline{PAPR} = \max(PAPR_1, PAPR_2, \dots, PAPR_{N_t}). \quad (3.5)$$

$$PAPR_p = \frac{\max_{0 \leq n < JK} |s_n^p|^2}{\frac{1}{JK} \sum_{n=0}^{JK-1} |s_n^p|^2}, \quad p = 1, 2, \dots, N_t. \quad (3.6)$$

where N_t is transmit antenna, $PAPR_p$ is the PAPR of transmit antenna p , and s_n^p is the discrete OFDM signal of transmit antenna p .

In case that selective mapping technique is used for PAPR reduction. We assume that the number of candidates for the selective mapping operation scheme is Q . The selector choose the candidate with the lowest \overline{PAPR} . In other words, a minimax criterion is used, which can be described as

$$(\underline{s}_1, \dots, \underline{s}_{N_t}) = \arg \min_{s_1, \dots, s_{N_t}} (\overline{PAPR}) \quad (3.7)$$

where $(\underline{s}_1, \dots, \underline{s}_{N_t})$ are transmitted OFDM symbols with lowest PAPR, and by Eqs.(3.6) $s_p = (s_{p,0}, \dots, s_{p,JK})$ which is time-domain signal for transmit antenna p .

3.4 CARI Scheme

We now describe the CARI scheme[3] with $N_t = 2$ based on the MIMO OFDM investigated in this chapter. It is easy to that C_i and $\pm C_i^*(i = a, b)$ have the same PAPR properties. Therefore, for the LDPC coded Alamouti scheme, the PAPR reduction needs to be done only for C_1 in equation Eqs.(3.1).

For CARI, we partition the C_a and C_b into W subblocks of equal sizes, denoted as

$$C_a = \begin{bmatrix} C_{a1} & C_{a2} & \cdots & C_{aW} \end{bmatrix} \quad (3.8)$$

$$C_b = \begin{bmatrix} C_{b1} & C_{b2} & \cdots & C_{bW} \end{bmatrix} \quad (3.9)$$

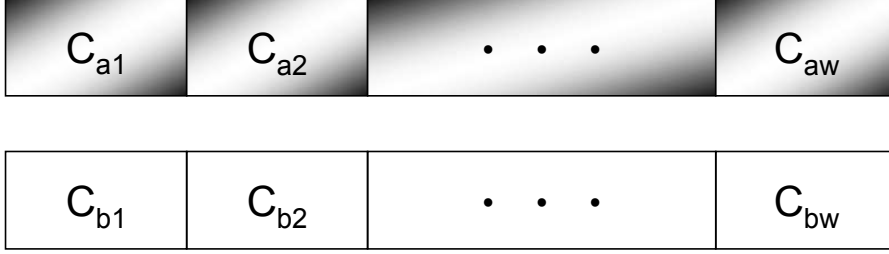


Figure 3.7: Partition of the C_a and C_b .

Each subblock has K/W elements in it as shown in Fig.(3.7). Now we perform anti-clockwise rotation and inversion across 2 antennas, which is shown in Fig.(3.8) and Table(3.2). That is, there are four kinds of candidates for each pair of C_{ai} and C_{bi} . With W subblocks and 2 antennas, 4^W candidates can be obtained. In case that

	Operation ($i = 0, 1, \dots, W$)
I	C_{ai} and C_{bi} are unchanged
II	C_{ai} and C_{bi} are swapped
III	C_{ai} and C_{bi} are inverted, i.e., $-C_{ai}$ and $-C_{bi}$
IV	C_{ai} and C_{bi} are swapped and inverted, i.e., $-C_{ai}$ and $-C_{bi}$ are swapped

Table 3.2: Four operations of each subblock.

M is large, this method will be impractical, since we have to search a large number of candidates to obtain the best PAPR. Hence, a suboptimal method is considered in [3], which is called Successive Suboptimal CARI (SS-CARI) scheme. The block diagram is shown in Fig.(3.9). At the beginning, the operations for C_{a1} and C_{b1} in Table(3.2) are executed. Then, PAPR values of the four candidates are calculated.

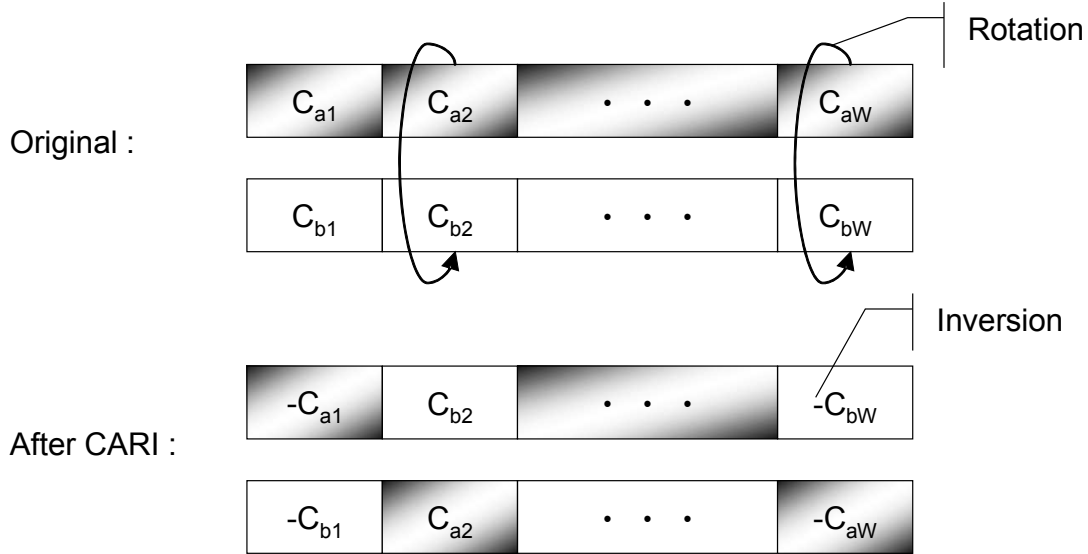


Figure 3.8: Cross-Antenna Rotation and Inversion (CARI) scheme.

For example, if the operation II has the lowest PAPR, the first subblock is fixed as shown in Fig.(3.10). Next, four operations for C_{a2} and C_{b2} are performed and the PAPR values of the four candidates are calculated. Again, the second subblock is fixed with the lowest PAPR. By proceeding this to all W subblocks, a total of $4W$ candidates can be obtained which is less than 4^W candidates in CARI scheme. Note that $S = 2W$ bits for side information are still needed for the SS-CARI.

In Section (3.5), we will propose a novel method to reduce the PAPR of MIMO-OFDM in time domain. To compare to the proposed time-domain scheme, we set the partition number to be $W = Q/4$ for SS-CARI, where $Q = 8, 16, \dots$ is the total number of candidates. In Fig.(3.9), we observe that the transmitter needs $2Q$ IFFT computations in order to obtain Q candidates. The proposed method described in Section (3.5) will need only two IFFT computations.

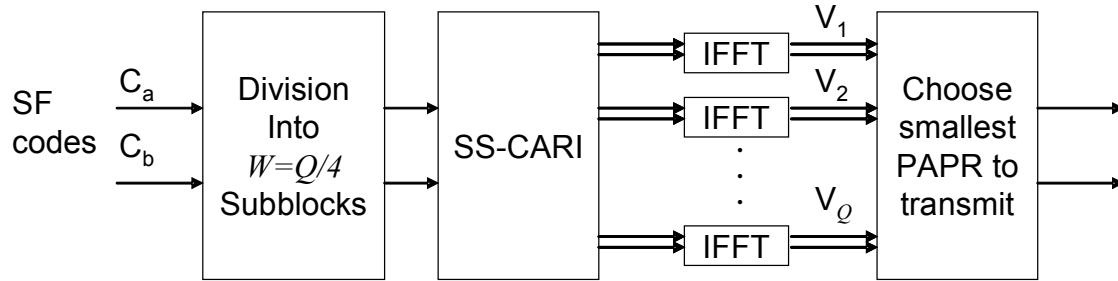


Figure 3.9: Block diagram of SS-CARI scheme.

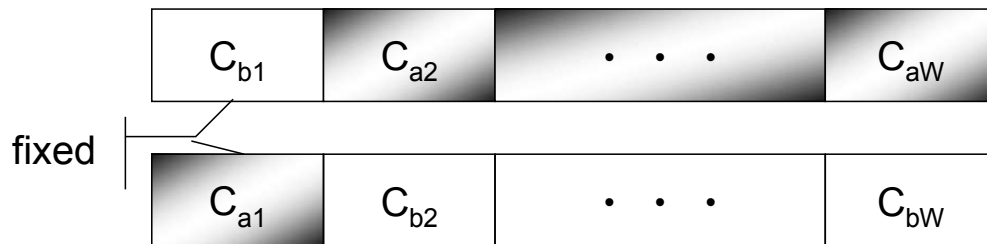


Figure 3.10: Successive Suboptimal Cross-Antenna Rotation and Inversion (SS-CARI) scheme.

3.5 Time-Domain Circular Shift Scheme

Now we will show our main result of this research that is Time-Domain Circular Shift Scheme (TDCS) for PAPR reduction in the MIMO-OFDM system.

3.5.1 Time-Domain Circular Shift Scheme

The time-domain circular shift (TDCS), which produces candidates in time-domain instead of in frequency domain, is depicted in Fig.(3.11). The time-domain OFDM

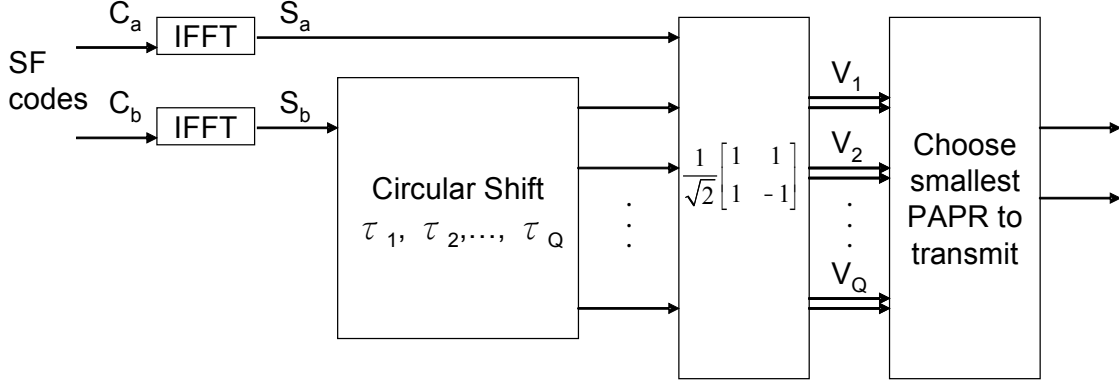


Figure 3.11: Time-domain circular shift (TDCS) scheme.

symbols for two transmit antennas are denoted as

$$S_a = \begin{bmatrix} S_{a1} & S_{a2} & \cdots & S_{a,JK} \end{bmatrix} \quad (3.10)$$

$$S_b = \begin{bmatrix} S_{b1} & S_{b2} & \cdots & S_{b,JK} \end{bmatrix} \quad (3.11)$$

We apply a circular shift³ with parameter τ_i on S_b ($i = 1, \dots, Q$). We denote the circular-shifted signals for parameter τ_i by \widehat{S}_b^i , where

$$\widehat{S}_b^i = \begin{bmatrix} \widehat{S}_{b1}^i & \widehat{S}_{b2}^i & \cdots & \widehat{S}_{b,JK}^i \end{bmatrix} \quad (3.12)$$

Then, we multiply the combination of S_a and \widehat{S}_b^i by a unitary matrix U to obtain a candidate for parameter τ_i . The i th candidate will be

$$V_i = \begin{bmatrix} V_a^i \\ V_b^i \end{bmatrix} = U \begin{bmatrix} S_{a1} & S_{a2} & \cdots & S_{a,JK} \\ \widehat{S}_{b1}^i & \widehat{S}_{b2}^i & \cdots & \widehat{S}_{b,JK}^i \end{bmatrix} \quad (3.13)$$

³A circular shift is a permutation of the entries in a tuple where the last element becomes the first element and all the other elements are shifted, or where the first element becomes the last element and all the other are shifted.

where V_a^i and V_b^i are the OFDM symbols for the first and the second transmit antennas respectively and,

$$U = \frac{1}{\sqrt{2}} \begin{bmatrix} 1 & 1 \\ 1 & -1 \end{bmatrix} \quad (3.14)$$

We have one candidate for each shift. Hence there are Q candidates in total. We use minimax criterion to find the lowest PAPR and transmitted OFDM symbols according to Eqs.(3.5) and Eqs.(3.7).

From Fig.(3.11) we observe that only *two* IFFT computations are needed and the number of bits for side information is $S = \log_2 Q$. Thus, TDCS can reduce the implementation complexity as compared to SS-CARI and is more applicable to practical systems.

3.6 Simulation Results

In this section, we provide the simulation results so that we can compare the performances of SS-CARI and the proposed TDCS regarding CCDF and BER (bit error rates).

3.6.1 CCDF Performance

In our simulation, 10^5 random OFDM sequences are generated to obtain the CCDF. We use $N_t = 2$ and $K = 128$ subcarriers. The modulation is QPSK. Oversampling factor J is set to 4..

Fig.(3.12) shows the CCDF of PAPR for the TDCS and SS-CARI scheme using

	$Q = 8$		$Q = 16$	
PAPR Scheme	Side Information S bits	IFFT Number ξ	Side Information S bits	IFFT Number ξ
TDCS	3	1	4	1
SS-CARI	4	8	8	16

Table 3.3: Comparison of information bit S and the number of IFFT needed ξ .

$Q = 8$ and $Q = 16$ candidates respectively. The proposed TDCS scheme for $Q = 8$ achieves better performance than the SS-CARI scheme for $W = 2$. The TDCS and SS-CARI schemes for $Q = 16$ perform almost the same. We list the number of needed side information bits and the number of needed IFFT computations for both TDCS and SS-CARI in Table(3.3). We can observe that both the side information S and the number of IFFT computations needed ξ for TDCS scheme are less than that for SS-CARI scheme.

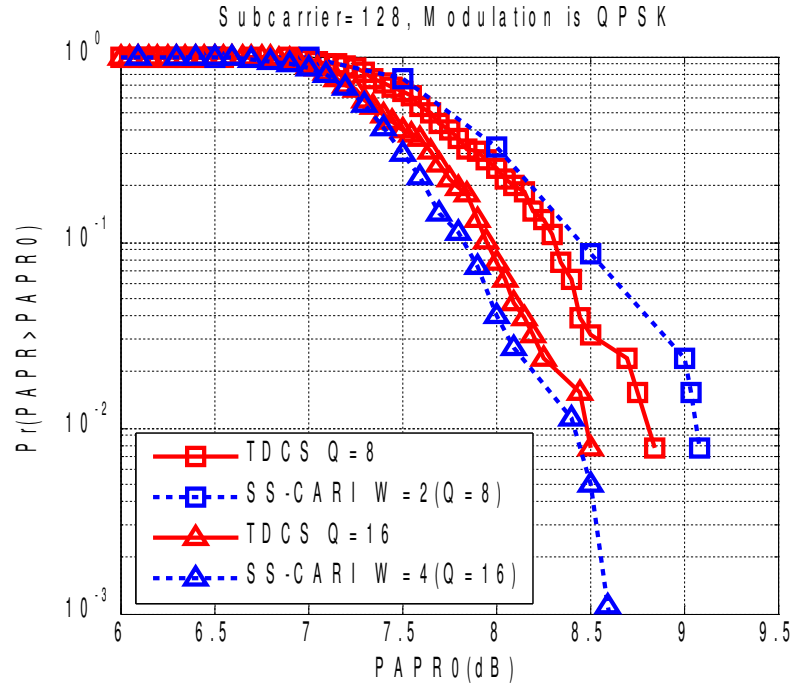


Figure 3.12: SS-CARI and TDCS scheme for different value of candidates Q .

3.6.2 BER Performance

In many PAPR research works, the effect on BER is neglected. In fact, the effect on BER may be great in some cases. In our simulation, we use $N_t = 2$ and $K = 256$ subcarriers. The available bandwidth is 1MHz and the subcarrier $K = 256$. We consider the channel with power delay profiles: COST207[22] typical urban six-ray power delay profile. The oversampling factor is $J = 4$. All the other parameters are just the same as what we use in Section (3.2).

Fig.(3.13) and Fig.(3.14) show the performance of SS-CARI and TDCS using the space frequency code investigated in Section (3.1). In the simulation, we assume that CSI and side information can be recovered correctly by the receiver. Take 7dB clipping ratio case as example. We can observe that the BER performance of both

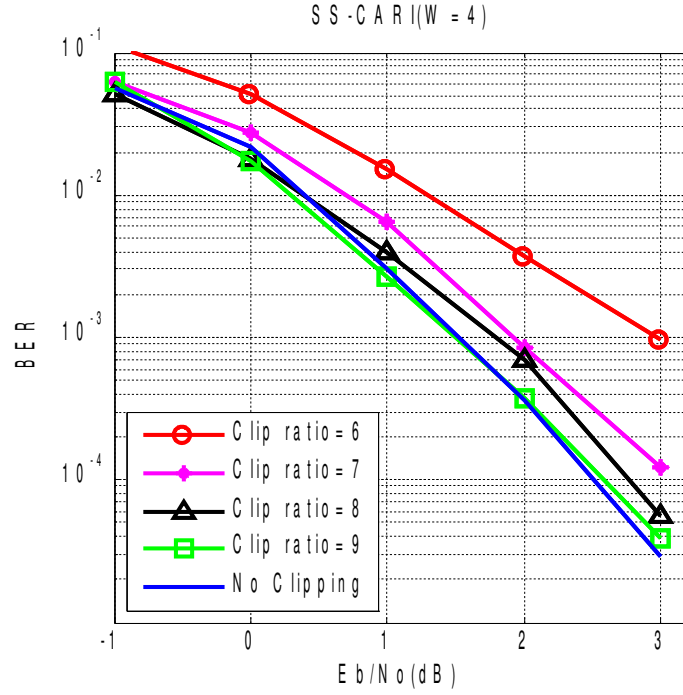


Figure 3.13: SS-CARI BER performance for $W = 4$.

schemes are around 10^{-4} at $E_b/N_0 = 3\text{dB}$.

In Eqs.(3.13), multiplying unitary matrix U to the left side of a space-frequency codeword will not effect the BER performance. Hence the U can be designed by any unitary matrix.

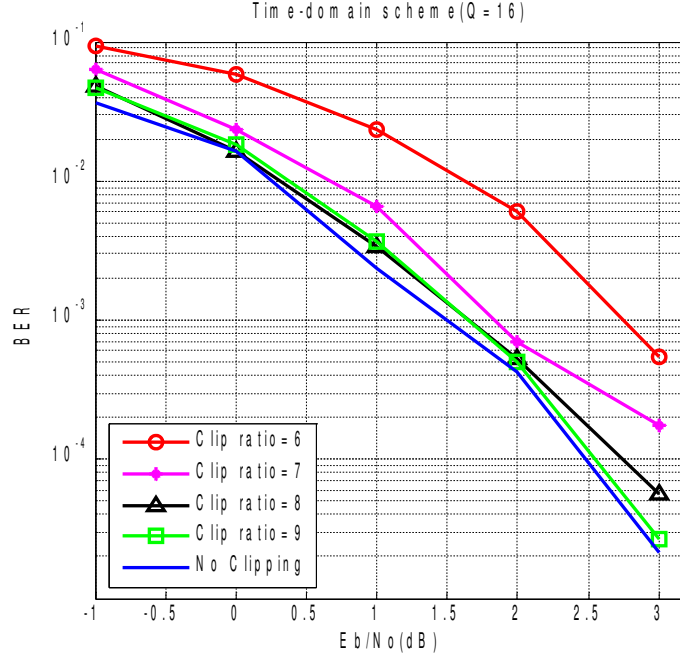


Figure 3.14: TDCS BER performance for $Q = 16$.

Side Information Embedded

In some situations, the side information is embedded into the system. There are many methods to embed the side information into the system. A major concern is that the side information must be well protected. Otherwise, serious error propagation will occur. Here, we consider a simple method which is obtained by inserting the side information into the zero terms of Eqs.(3.1) and Eqs.(3.2) and each reserved subcarrier contains one side information bit. In fact, we can insert more than one bit to one subcarrier if the system needs a large number of the side information bits. In order to protect the side information bit, the power of side information signals is transmitted four times of original signals. The performance of SS-CARI scheme remain similar to TDCS scheme, shown in Fig.(3.15) and Fig.(3.16). Take the 7dB

clipping ratio condition as example, we can observe that the BER performance of both schemes are around 10^{-4} at $E_b/N_0 = 3\text{dB}$. That is, the system suffers no BER performance degradation by inserting the side information bits in the simple methods described above.

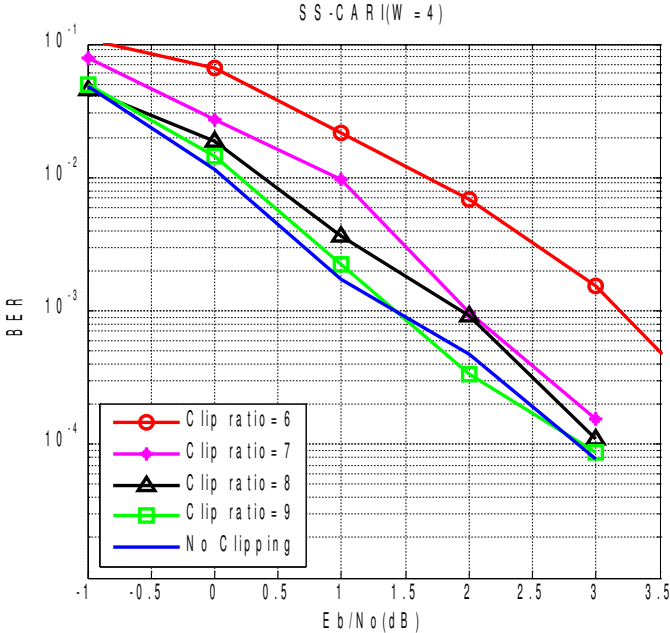


Figure 3.15: SS-CARI BER performance for $W = 4$ with side information embedded.

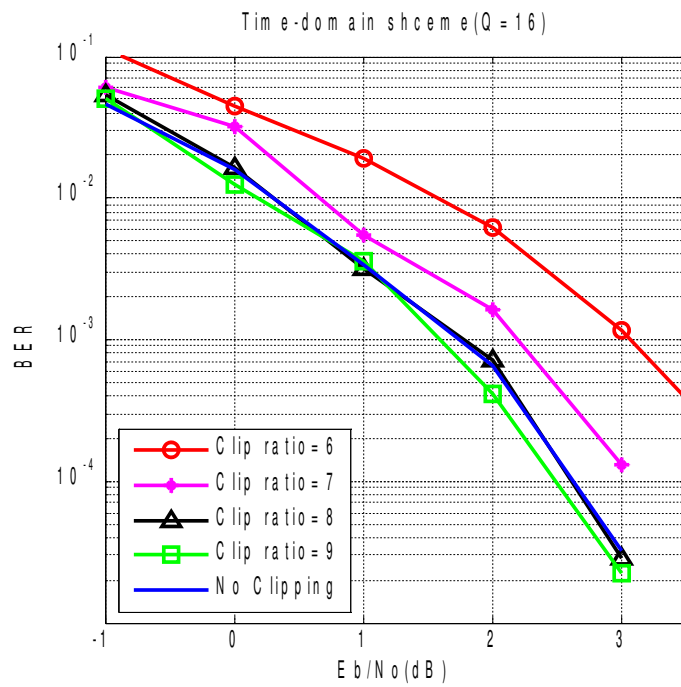


Figure 3.16: TDCS BER performance for $Q = 16$ with side information embedded.

Chapter 4

Extending The Linear Range of Power Amplifiers with Precoding

In this chapter, the research work about subproject 3 regarding “ extending the linear range of power amplifiers with precoding ” is briefly reported. In the first year of the project, we investigate the idea of using Dirty Paper Coding (DPC) to extend the linear range of power amplifiers (PAs) for the single input single output (SISO) single carrier case. In addition, we also study the effect of peak to average power ratio (PAPR) constraint on the diversity-multiplexing (DM) tradeoff of multiple input multiple output (MIMO) channel. After this issue is addressed, we develop a method that can reduce the PAPR of MIMO single carrier systems without sacrificing the optimality of DM tradeoff.

4.1 Extending the Linear Range of Power Amplifiers with DPC

In this project we propose a novel solution to extend the linear range of a given PA with precoding. The idea behind the proposed method is based on the well known information theoretic result on interference cancellation at the transmitter. In the monumental work by Costa [4], it was proven that if the interference in the channel is known to the transmitter, cancellation of the interference can be done at the transmitter without increasing the transmission power. As a result, the clean channel capacity can be achieved as if the interference does not exist. Since this technique stems from a completely different philosophy than that of the PAPR reduction and the PA linearization methods, the proposed method can be combined with any of these conventional remedies to achieve linear range extension and PAPR reduction at the same time. Additionally, the proposed method can be combined with the cancellation of channel interferences as a unified precoder with small overhead. Before Costa's theoretical result, a practical coding structure had already been applied to the inter-symbol interference channel by Tomlinson [23] and Harashima [24]. A few decades later, Erez et al. improved and generalized the Tomlinson Harashima precoding (THP) for the general interference channel [25]. The coding structure they proposed realizes Costa's theoretical result on "writing on dirty paper". Therefore, this coding structure is called DPC. Compared with the well known THP which can also remove the interference at the transmitter under the

same average power constraint, DPC has several advantages in avoiding the shaping loss, power loss, and modulo loss.

To apply the above DPC interference cancellation to a communication system with a nonideal PA, we can treat the distortion caused by the PA as an additive interference. In general, the PA transfer function is known to the transmitter by, for example, online measurement. Thus the distortion can be determined and removed at the transmitter through DPC. As a result the amplitude of the data-carrying signal is allowed to exceed the linear range of the PA. At the receiver, the signal is received as if there was no PA distortion at all. The end result is an extended PA linear range. Such a precoding technique seemingly implies that one could use an arbitrarily large signal amplitude to achieve high channel capacity while the transmission power at the output of the PA is still bounded. We found that this is not the case due to the reason that in this scenario the interference is directly related to the DPC outcome. Therefore, a special attention has to be paid to the relation between the DPC and the interference. In other words, the precoding scheme has to make sure that the interference used in DPC is exactly the distortion due to PA clipping. Otherwise cancellation of the interference will not be possible.

Summary of Results

In Fig.(4.1) the system model of the proposed precoding scheme is shown. After channel coding, the signal to be transmitted goes through a combined shaping and DPC module. Differing from regular DPC, the "interference" to be cancelled here

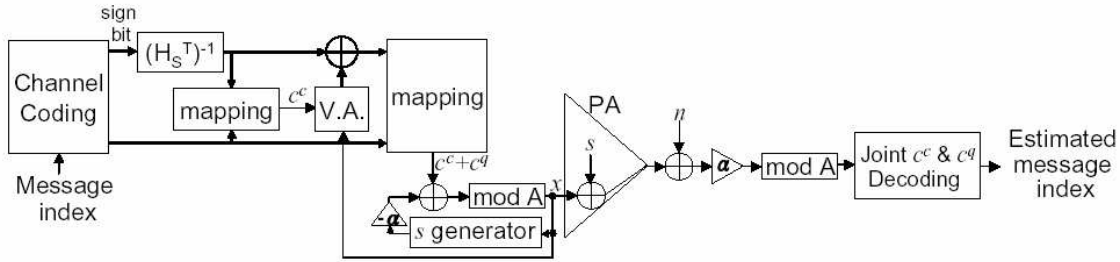


Figure 4.1: The system model for the proposed precoding scheme.

is the PA clipping noise which is dependent of the shaped signal. Thus, there is no guarantee that a valid "interference" matching the shaping output and the clipping effect exists. Detailed analysis of the existence of a valid interference can be found in the full report.

To validate the proposed idea, we compare through simulation the BER versus SNR performance of the proposed scheme with a system without precoding for different minimum distances. The SNR is defined as the ratio of the energy at the PA output to the noise variance at the receiver. Both systems have channel coding and constellation shaping to acquire coding gain and shaping gain. The constellation size we use is 64-QAM. The code length is 128. A rate 1/2 convolutional code with generator $[7, 5]_8$ is used for the sign bit shaping. It has an inverse syndrome former $(H_s^T)^{-1}$ with generator $[1, 3]_8$. A rate 1/5 convolutional code with generator $[37, 27, 33, 25, 35]_8$ is used for the channel coding. The linear range of PA is set as 0.3.

The simulation result is shown in Fig.(4.2). Scale 0.48 represents that the four corner points of the 64-QAM constellation are exactly on the boundary of the linear

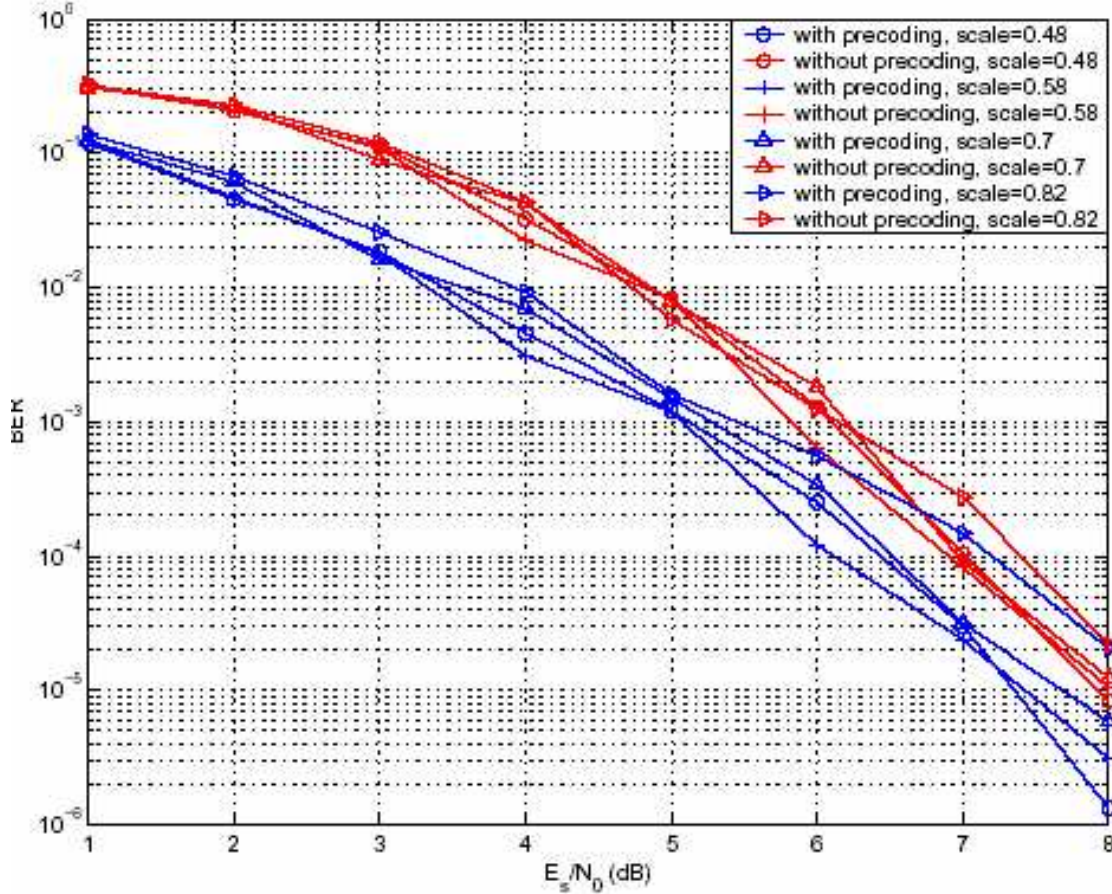


Figure 4.2: BER versus SNR for the proposed precoding scheme and systems without precoding with different minimum distances.

range. The minimum distance and the number of points outside the linear range increases with the increasing scale. From the simulation we can find that the proposed precoding scheme provides gains about 0.8-dB and 0.6-dB at $\text{BER} = 10^{-4}$ and $\text{BER} = 10^{-5}$ respectively over the system without precoding. The gain becomes larger with decreasing SNR because the area of the extended linear range increases with decreasing SNR and the proposed scheme can prevent more clipping interference. For systems without precoding, as the scale starts increasing, the gain

from the increased minimum distance of points within the linear range can compensate the performance degradation caused by points outside the linear range. Due to shaping, only a small portion of all the constellation points are clipped. The shaping operation makes the distribution of the constellation approximately Gaussian, i.e., constellation points with less energy occurring more frequently than those with higher energy. Thus the probability of clipping is reduced. When more points are outside the linear range, for example, when $\text{scale}=0.82$, the errors can no longer be compensated by the gain from the increased minimum distance and the BER increases. On the other hand, for the proposed system, because the area of extension decreases with increasing SNR, the effect of precoding becomes less significant. As a result, the performance of the proposed precoding scheme approaches to that of systems without precoding when the scale and the SNR are both high. Thus we can find that at $\text{scale}=0.82$ the BER curves of both cases approach to each other much more with increasing SNR than those of other smaller scales. This condition shows that the gain from increasing the minimum distance is small when SNR is high.

4.2 PAPR Reduction of Space-Time Codes That Achieve D-MG Tradeoff

A result of Zheng and Tse [26] states that over a quasi-static channel, there exists a fundamental tradeoff known as diversity-multiplexing gain (D-MG) tradeoff. The quest for space-time codes that achieve D-MG tradeoff has generated numerous

works. However, these space-time codes generally have a pretty high PAPR on each antenna. In a realistic system, to avoid inefficiently operating the power amplifier; one should put constraints on PAPR. In this context, we investigate D-MG tradeoff with PAPR constraints. The results show D-MG tradeoff remains the same even with PAPR constraints, but space-time codes devised to achieve D-MG tradeoff need some modifications to meet the PAPR constraints. Therefore, we propose two general ways to reduce PAPR without affecting codes structure and without any side information being transmitted. They are both based on constellation shaping, that is, a constellation is used such that the transmitted signals have low PAPR values. The first method is similar as [27] except we choose the Hermite Normal Form (HNF) decomposition instead of Smith Normal Form (SNF); the second one takes the idea of integer reversible mapping [28]. If the approximate cubic shaping is used, both techniques would lead to an asymptotical PAR value equal to 3 when SNR is large.

4.2.1 Approximate Cubic Shaping for D-MG Tradeoff Codes

Here we focus on the shaping on a general space-time code X in the form of

$$x = Gs \quad x, s \in \mathbb{Z}^N \quad (4.1)$$

where x is the vector representation of X . Although existing shaping algorithms give a pretty good shaping gain with limited PAPR, they require x chosen from Cartesian product of QAM. If $G \neq I$, we do not know if x exceeds the PAPR constraint until s is chosen. That makes the complexity of shaping extremely large. Therefore, it is

difficult to directly apply existing algorithms to x . To avoid this problem, consider a set of perturbations u_i , such that

$$x = G(s + u_i) = Gs + Gu_i = s' + u'_i \quad (4.2)$$

$$u'_i = [\varepsilon_1, \varepsilon_2, \dots, \mu_i, \dots, \varepsilon_N]^T, \quad |u_i| \gg |\varepsilon_j| \quad (4.3)$$

then when we want to choose u_i , $i = 1, 2, \dots, N$ to minimize $|x|^2$ with limited PAPR, it is easy to exclude some u_i , of which μ_i exceeds the peak constraint, thus saving lots of complexity. We call this shaping “approximate cubic shaping”, since when $\varepsilon_i = 0$, we can view it as the cubic shaping. After the approximate cubic shaping is done, we may apply trellis shaping to x . Therefore, in the following we mainly focus on how to do the approximate cubic shaping.

Cubic Shaping via Hermite Normal Form (HNF) Decomposition

Consider a partition \mathbb{Z}^N/Λ , where $\Lambda = Q\mathbb{Z}^N$, the elements in Q are integer, such that

$$GQ = \sigma I \quad \det(Q) \cong \sigma^N \quad (4.4)$$

$$\sigma^N = \text{total rates} \quad (4.5)$$

For any coset $s + Q\mathbb{Z}^N$,

$$\begin{aligned} x &= G(s + Q\mathbb{Z}^N) = Gs + GQ\mathbb{Z}^N \\ &= s' + GQ\mathbb{Z}^N \cong s' + \sigma\mathbb{Z}^N \end{aligned}$$

If we choose $Q = \text{round}(\tilde{\sigma}G^{-1}) \geq \sigma^N$

$$u_i = Qe_i, \quad e_i \in \{[0, 0, \dots, \mathbb{Z}_i, \dots, 0]^T\} \quad (4.6)$$

when σ is large,

$$\begin{aligned} x &= s' + GQe_i \\ &= s' + v_i \\ &\cong s' + \sigma e_i \end{aligned}$$

where $v_i \in \{[\varepsilon_1, \varepsilon_2, \dots, \sigma\mathbb{Z}_i, \dots, \varepsilon_N]^T\}$.

The main challenge is how to find the coset leaders, namely, indexing. We can formulate the problem as: find a cosetleader $s \in S$, such that

$$\text{if } s^i \neq s^j \quad \text{where } s^i, s^j \in S \quad (4.7)$$

$$\text{then } s^i \neq s^j + Qz^N \quad \text{where } z^N \in \mathbb{Z}^N \quad (4.8)$$

If $Q = D = \text{diag}(d_1, d_2, \dots, d_N)$, it is natural to choose coset leader $s \in S$ where

$$s = [s_1, s_2, \dots, s_N]^T \quad (4.9)$$

$$S = \{s | 0 \leq s_i < d_i\} \quad (4.10)$$

If $Q = UDV$, where U, V is unimodular, (i.e. integer entry, $\det(U) = \pm 1, \det(V) = \pm 1$). Since

$$s + D\mathbb{Z}^N = s + D(V\mathbb{Z}^N) \quad (4.11)$$

Then

$$\begin{aligned} Us + UDV\mathbb{Z}^N &= Us + Q\mathbb{Z}^N \\ &= \hat{s} + Q\mathbb{Z}^N \end{aligned} \quad (4.12)$$

The question is the existence of decomposition for Q . Fortunately, this kind of decomposition indeed exists [29]. We repeat here for completeness.

Theorem 9 *Any integer matrix Q can be decomposed into $Q = UDV$ where U, V are unimodular matrices and D is diagonal matrix such that $d_1|d_2|\dots|d_N$.*

We call the matrix D as the Smith Normal Form (SNF) of the matrix. If the SNF decomposition of the matrix is given, the encoding algorithm for the shaped constellation can be represented by

$$\begin{aligned}\hat{s} &= Us \\ \alpha &= \lfloor Q^{-1}\hat{s} \rfloor \\ \tilde{s} &= \hat{s} - Q\alpha\end{aligned}\tag{4.13}$$

Since \hat{s} in Eqs.(4.12) is not necessary in the parallelotope enclosed by the columns of Q when $V \neq I$, we need to do the modulo operation in Eqs.(4.13). The decoding algorithm can be represented by

$$\begin{aligned}\check{s} &= U^{-1}\tilde{s} = [\check{s}_1, \check{s}_2, \dots, \check{s}_N]^T \\ s_i &= \check{s}_i \text{ mod } d_i\end{aligned}\tag{4.14}$$

Examine the algorithms, we will find some unnecessary constraints on SNF decomposition. If we decompose $Q = RV$, where V is unimodular and R is lower triangular, then

$$\begin{aligned}s + Q\mathbb{Z}^N &= s + R(V\mathbb{Z}^N) \\ &= s + R\mathbb{Z}^N\end{aligned}\tag{4.15}$$

Let $r_{ii} \neq 0$ be the diagonal element of R , we can identify coset leaders $s \in S$ where

$$s = [s_1, s_2, \dots, s_N]^T$$

$$S = \{s | 0 \leq s_i < r_{ii}\}$$

There is also a theorem that guarantees the existence of the decomposition of $Q = RV$. We call the matrix R as Hermite Normal Form (HNF) [30].

Theorem 10 *Any square nonsingular integer matrix Q can be decomposed into $Q = RV$ where V is unimodular matrix and R is lower triangular matrix with integer entries.*

Similarly, approximate cubic shaping can also be done via integer reversible matrix mapping [28].

4.2.2 Numerical Results

Avg. power	Peak power	PAPR
670.25	5771.86	8.61
670.24	5900.41	8.80
670.27	5689.12	8.49
670.28	5677.71	8.47
670.35	5433.56	8.11

Table 4.1: Without shaping.

Avg. power	Peak power	PAPR
716.18	2643.67	3.67
703.88	2674.64	3.80
707.42	2796.07	3.95
698.39	2440.64	3.49
700.75	2476.54	3.53

Table 4.2: After shaping.

As an example, we consider a 5×5 MIMO system. Symbols at each antenna are drawn from 64 QAM, we choose the perfect space-time code in [31], using the HNF shaping method.

We observe that PAPR value is about 3 after shaping; it will approach 3 as the constellation becomes even larger. The increased average power is due to the rounding operation we take. Similarly, when the constellation is large enough, the increased power will be relative small.

Chapter 5

Conclusions and Remarks

It is well recognized that MIMO-OFDM (multiple-input multiple output orthogonal frequency division multiplexing) [1] is a promising technique for achieving broadband transmission over possibly frequency selective fading channels. Prof. Hsiao-Feng Francis Lu of Department of Communication Engineering, National Chung-Cheng University, Prof. Hsuan-Jung Su of Graduate Institute of Communication Engineering, and Department of Electrical Engineering, National Taiwan University and I (Mao-Chao Lin, Graduate Institute of Communication Engineering and Department of Electrical Engineering, National Taiwan University) jointly conduct a three-year project beginning August 1 of 2007 for investigating a core issue of MIMO-OFDM, i.e., the coding and modulation of MIMO OFDM. Prof. Hsiao Feng Francis Lu is responsible for the first subproject titled “Optimal Coding and Modulation Designs for the Fourth Generation Mobile Communication systems under various MIMO-OFDM Channels.” Prof. Hsuan-Jung Su is responsible for the third subproject

titled “Extending the Linear Range of Power Amplifiers with Precoding.” I, myself, is responsible for the second subproject titled ‘MIMO OFDM Systems with Low PAPR and Error Rates.’”

In the first year of this three-year research, we have many interesting results.

For the first subproject, we are concerned with the optimal constructions of space-frequency codes under various MIMO-OFDM channels and two major results will be reported. The first result is an optimal construction of space-frequency codes based on the pairwise error probability (PEP) criterion. This result will be published in *IEEE Transactions on Information Theory*, vol. 53, no. 5, 2007 as a *regular paper*. While the first result considers the notion of optimality of space-frequency codes from the angle of PEP analysis, the second one focuses more on the codeword error probability point of view. The diversity-multiplexing gain tradeoff (DMT) proposed by Zheng and Tse [2] has been shown to be a powerful tool in analyzing the performance tradeoff of space-time codes when the channel is modeled as a quasi-static Rayleigh fading channel. On the other hand, there is almost no known results for the MIMO-OFDM channel, which is in fact a more practical channel and has wide applications in wide-band communication standards, especially the most important 4G mobile communication. We take a first step by considering the SIMO-OFDM channel and analyze the corresponding DMT. A systematic construction of SIMO-OFDM space-frequency codes meeting the DMT is also provided, which can also be applied to all OFDM-based communication schemes and yield the optimal performance.

For the second subproject, we have completed the investigation of an efficient MIMO-OFDM system, which is constructed by the concatenation of LDPC coding and Alamouti coding. Then, we propose a low-complexity PAPR reduction technique for the investigated SF code, which is a kind of selective mapping technique implemented on the time-domain.

For the third subproject, we investigate the idea of using Dirty Paper Coding (DPC) to extend the linear range of power amplifiers (PAs) for the single input single output (SISO) single carrier case. The proposed method can be combined with any of these conventional remedies to achieve linear range extension and PAPR reduction at the same time. Additionally, the proposed method can be combined with the cancellation of channel interferences as a unified precoder with small overhead. In addition, we also study the effect of peak to average power ratio (PAPR) constraint on the diversity-multiplexing (DM) tradeoff of multiple input multiple output (MIMO) channel. We develop a method that can reduce the PAPR of MIMO single carrier systems without sacrificing the optimality of DM tradeoff.

Some of the results given in this report are very significant and have been accepted for publication in the prestigious academic journal such as IEEE Transactions on Information Theory. Some of the results given in this report are still in the primitive form and can be expanded to more fruitful results. In the next two years, the primitive results together with items listed in the proposal for the last two years will be further investigated. Integration of the individual results in the subprojects will also be implemented.

Bibliography

- [1] G. Raleigh and J. M. Cioffi. "Spatio-temporal coding for wireless communications". *in Proc. IEEE GLOBECOM*, pages pp. 1809–1814.
- [2] L. Zheng and D. Tse. "Diversity and multiplexing: a fundamental tradeoff in multiple antenna channels". *IEEE Trans. Inform. Theory*, vol. 49(no. 5):pp.1073–1096, May. 2003.
- [3] Z.Latinovic M. Tan and Y.Bar-Ness. "STBC MIMO-OFDM Peak Power Reduction by Cross-Antenna Rotation and Inversion". *IEEE commun. Lett.*, 9:592–594, Jul. 2005.
- [4] M. H. M. Costa. "Writing on dirty paper". *IEEE Trans. Inform. Theory*, Vol.29:pp. 439–441, May. 1983.
- [5] B. Lu and X. Wang. "Space-time code design in OFDM systems". *Proc. IEEE 2000 GLOBECOM*, pages pp. 1000–1004, Nov. 2000.
- [6] M. Olfat W. Su, Z. Safar and K. J. Liu. "Obtaining full-diversity space-frequency codes from space-time codes via mapping". *IEEE Trans. Signal*

- Processing*, vol. 51(11):pp. 2905–2916, Nov. 2003.
- [7] N. Seshadri V. Tarokh and A. R. Calderbank. "Space-time codes for high data rate wireless communication: Performance criteria and code construction". *IEEE Trans. Inform. Theory*, pages 744–764, Mar. 1998.
- [8] P. V. Kumar H. F. Lu, Y. Wang and K. M. Chugg. "Remarks on space-time codes including a new lower bound and an improved code". *IEEE Trans. Inform. Theory*, pages pp. 2752–2757, Oct. 2003.
- [9] Y. Xin Z. Lin and G. Giannakis. "Space- time- frequency coded OFDM over frequency- selective fading channels". *IEEE Trans. Signal Processing*, vol. 50(10), Oct. 2002.
- [10] Branka Vucetic and Jinhong Yuan. "Space-time coding".
- [11] B. S. Rajan U. Sripati and V. Shashidhar. "Full-diversity group space-time-frequency (GSTF) codes from cyclic codes". *Proc. 2005 IEEE Int. Symp. Inform. Theory*, Sep. 2005.
- [12] V. Shashidhar U. Sripati and B. S. Rajan. "Designs and full-rank STBCs from DFT domain description of cyclic codes". *Proc. 2004 IEEE Int. Symp. Inform. Theory*, June 27 - July 2 2004.
- [13] H. F. Lu and P. V. Kumar. "Rate-diversity tradeoff of space-time codes with fixed alphabet and optimal constructions for PSK modulation". *IEEE Trans. Inform. Theory*, pages pp. 2747–2751, Oct. 2003.

- [14] F. J. MacWilliams and N. J. A. Sloane. "The Theory of Error-Correcting Codes". . *Amsterdam: North-Holland*, 1977.
- [15] S. G. Vladut M. A. Tsfasman and T. Zink. "Modular curves, Shimura curves and Goppa codes better than the Varshamov-Gilbert bound". *Math. Nachrichtentech.*, vol.109:pp. 21–28, 1982.
- [16] E. Gabidulin. "Theory of codes with maximum rank distance". *Problems of Information Transmission*, vol.21:pp. 3–16, Jan. - Mar. 1985.
- [17] E. Telatar. "Capacity of multi-antenna Gaussian channels". *Europ. Trans. Telecomm.*, vol. 10(no. 6):pp. 585–595, Nov.-Dec. 1999.
- [18] L. Gropop and D. Tse. "Diversity/multiplexing tradeoff in isi channels". *Proc. 2004 IEEE Int. Symp. Inform. Theory*, page pp. 97, Jul. 2004.
- [19] S. A. Pawar P. V. Kumar P. Elia, K. R. Kumar and H.-F. Lu. "Explicit construction of space-time block codes achieving the diversity-multiplexing gain tradeoff". *IEEE Trans. Inform. Theory*, vol.52(9):pp. 3869–3884, Sep. 2006.
- [20] H. F. Lu. "Explicit constructions of multi-block space-time codes that achieve the diversity-multiplexing tradeoff". *Proc. 2006 IEEE Int. Symp. Inform. Theory*, pages pp. 1149–1153, Jul. 2006.
- [21] J.Speidel S.ten Brink and R.Yan. "Iterative demapping and decoding for multilevel modulation". *in Proc. GLOBECOM*, pages 579–584, Nov. 1998.
- [22] G. Stuber. "Principles of Mobile Communication". 2001.

- [23] M. Tomlinson. “New automatic equalizer employing modulo arithmetic”. *Electr. Lett.*, Vol.7:pp. 138–139, Mar. 1971.
- [24] M. Miyakawa and H. Harashima. “A method of code conversion for a digital communication channel with intersymbol interference”. *Trans. Inst. Elec. Comm. Eng. Japan*, Vol.52-A:pp.272–273, Jun. 1969.
- [25] S. Shamai U. Erez and R. Zamir. “Capacity and lattice strategies for canceling known interference”. *in Proc. ISITA*, 2000.
- [26] L. Zheng and D. N. C. Tse. “Diversity and multiplexing: A fundamental trade-off in multiple antenna channels”. *IEEE Trans. Inf. Theory*, Vol.49(No.5):pp. 1073–1096, May. 2003.
- [27] HK Kwok Shape up: peak-power reduction via constellation shaping 2001 University of Illinois at Urbana-Champaign.
- [28] P. Hao and Q. Shi. “Matrix factorizations for reversible integer mapping”. *IEEE Trans. Signal Processing*, Vol.49:pp. 2314–2324, Oct. 2001.
- [29] H. J. S. Smith. “On systems of linear indeterminate equations and congruences”. *Phil. Trans. Roy. Soc. London*, 151:293326,, 1861.
- [30] C. Hermite. “Sur l’introduction des variables continues dans la theorie des nombres.”. *J. Reine Angew. Math.*41:191-216,, 1851.

- [31] Bharath Sethuraman Petros Elia and P. Vijay Kumar. “Perfect space time codes with minimum and non-minimum delay for any number of antennas”. *preprint, submitted to arXiv:cs.IT*, Vol.1(No.6), Dec. 2005.